FINAL REPORT
DOE Project DE-FC36-00CH11032

Diagnostics and Control of Natural Gas Fired Furnaces via Flame Image Analysis using Machine Vision & Artificial Intelligence Techniques

DOE-HQ Project Manager: Gideon Varga

Principal Investigator: Shahla Keyvan
University of Missouri-Columbia

Contributors: Handy Cokrojoyo, Dong Li, Rodney Rossow, Carlos Romero

Subcontractors: Lehigh Energy Research Center, R. E. Moore and Associates

December 2005

FINAL REPORT
DOE Project DE FC36-00CH11032

Project Title:	**Diagnostics and Control of Natural Gas Fired Furnaces via Flame Image Analysis using Machine Vision & Artificial Intelligence Techniques**
Report period:	**February, 2000 - December 31, 2004**
Principal Investigator:	Shahla Keyvan, University of Missouri-Columbia (Keyvan@missouri.edu)
Subcontractors:	Lehigh Energy Research Center R. E. Moore and Associates
Project Managers:	**DOE-HQ:** Gideon Varga **DOE Golden Field Office:** Debo Aichbhaumik, Paul Bakke **DOE Idaho Office:** David Herrin **DOE Chicago Office:** Edward Gallagher

OBJECTIVES

A new approach for detection of real-time properties of flames was used in this project to develop sensors to improve diagnostics and controls for natural gas fired furnaces. Camera images along with advanced image analysis and artificial intelligence techniques were used to provide high speed virtual sensors suitable for integration with the plant control system. The output of these sensors provides guidance for balancing air/fuel ratios. Identifying and correcting fuel rich burners would result in improved fuel efficiency. It is anticipated that this on-line diagnostic and control system will offer great potential for improving furnace thermal efficiency, lowering NO_x and carbon monoxide emissions, and improving product quality.

This project addresses the need for improved diagnostics and burner-balancing control of natural gas fired glass furnaces in order to improve fuel efficiency and reduce emissions. The project involved two Phases. Phase I was a feasibility study with one year duration and was completed in February 2001. Phase II, focused on burner control integration and was completed in December 2004.

PHASE I : Feasibility Study	**February 2000-February 2001**
PHASE II : Burner Control System Integration	**February 2001-December 2004**

This report starts with a summary of accomplishments during phase I (February 2000- 2001) followed by a summary of accomplishments during each year of phase II (February 2001-December 2004).

SUMMARY OF ACCOMPLISHMENTS DURING PHASE I

Phase I activities included: 1) Camera and spectrometer equipment selection and acquisition, 2) Data acquisition at a pilot-scale glass furnace in Rolla, Missouri, and at a research combustion facility in Pennsylvania, 3) spectroscopic data analysis and temperature calculation based on black body radiation model, and 4) Flame image analysis including image processing and feature extraction and classification by two ART neural network algorithms. At the end of Phase I a flame classification simulation game was developed as a marketing tool.

Highlight of Phase I activities:

- **Equipment Acquisition:**
  - Periscope, camera, Spectrometer, computer, and laptop
- **Data Acquisition:**

  Several experiments were performed for collecting data using both spectrometer and camera at the following two laboratory scale furnaces.

  1. Pilot Scale Glass Furnace, at the University of Missouri-Rolla (UMR)
  2. Combustion facility, at the Penn State University
- **Flame Image Analysis Encompassing Two Processes:**

  1. Image Processing
  2. Feature (flame characteristics) Extraction
- **Image Classification using Two Neural Network Paradigms:**

  1. Fuzzy ARTMAP (a supervised network)
  2. ART2-A (unsupervised network)
- **Simulation Game :**

  A simulation game module was also developed for demonstration of the concept. Figure 1 shows the cover page of this module which can be played on the web using JAVA Media Frame Player and is currently located at:
  http://www.missouri.edu/~keyvans/public_html/demo/cover.html

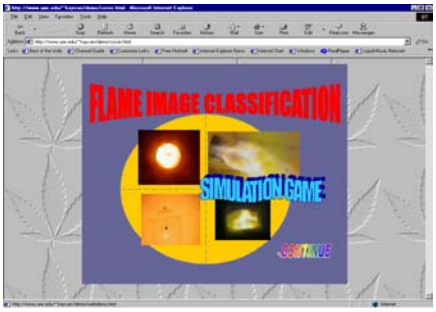

Figure 1. Cover page of the simulation game module

Pilot Scale Glass Furnace

This pilot scale furnace was a 0.16 Million Btu/hr glass furnace designed to carry out simulation and parametric studies of industrial glass tanks. The burner of this furnace was of the diffusion flame type, typically used in glass furnace applications. The furnace was controlled using a Labview hardware and software control system. Figure 2 shows the equipment set-up at this furnace. Figure 3 shows the computer screen of the furnace Labview software.

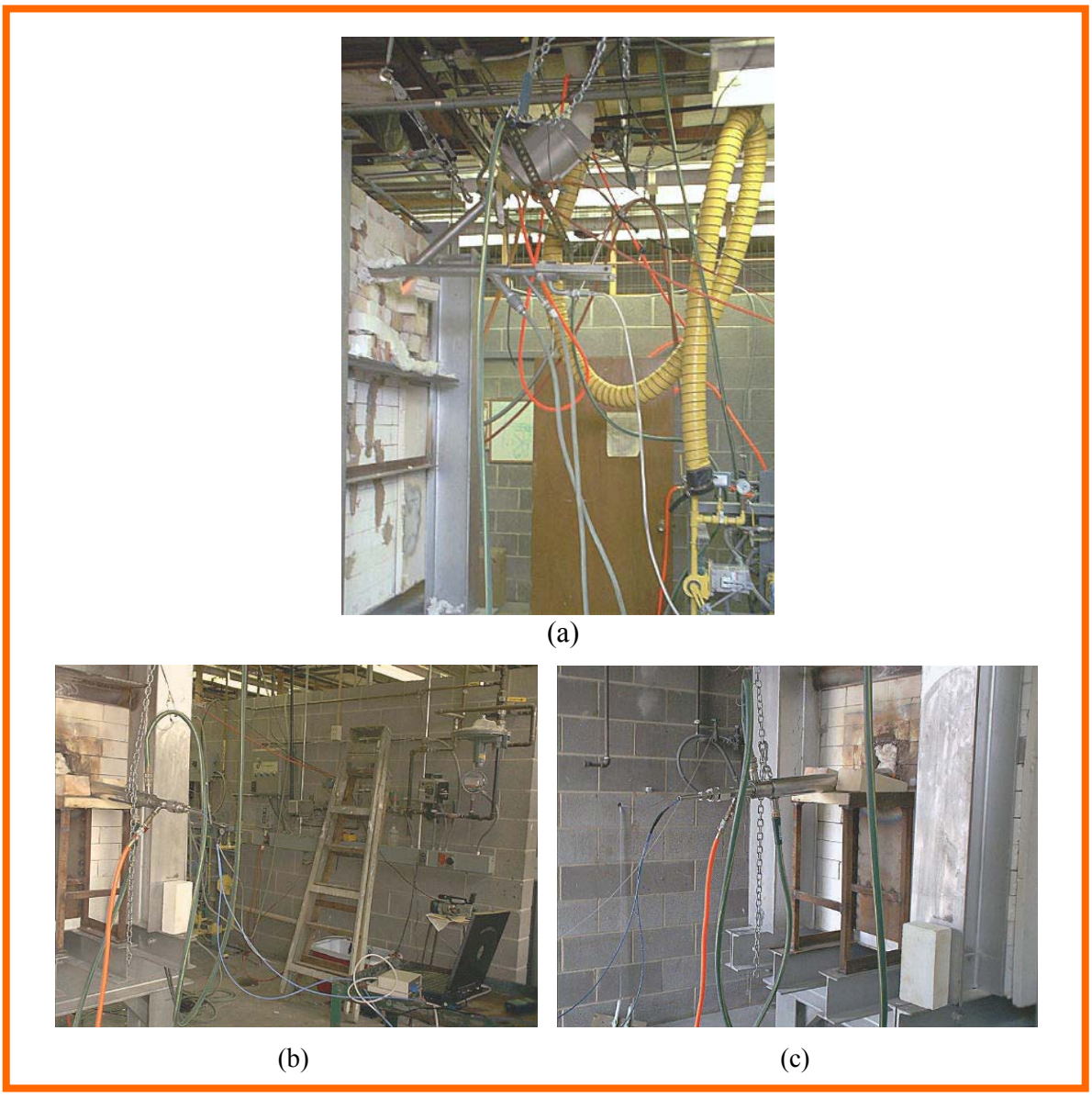

(a)

(b)

(c)

Figure 2. Equipment set-up at the pilot scale glass furnace. (a) Camera and flue gas equipment, (b) Spectrometer and computer, (c) Water/Air-cooled probe mounting set-up

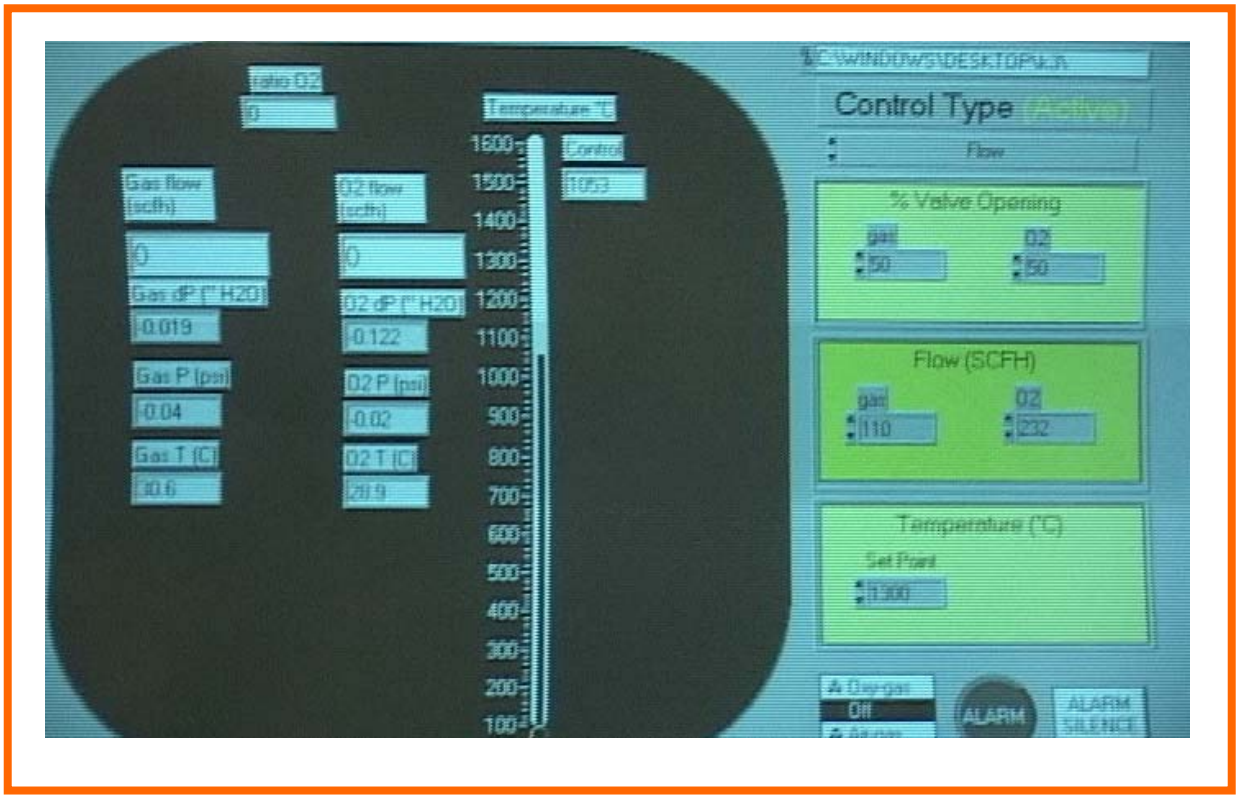

Figure 3. A computer screen of the Labview control system software

Combustion Facility

Combustion experimentations were conducted using a 2 Million Btu/hr combustion facility (see Figure 4) at the Pennsylvania State University in September and October 2000. The objective was to perform tests on a single burner, natural gas/air-fired combustor to obtain flame images and flame spectral radiation information under a range of burner operating conditions.

The combustor was fired by a single swirl burner. This burner allowed adjustment of air to fuel ratio and secondary to tertiary air ratio which affects burner stoichiometry, mixing rate and secondary air swirl. To promote and enhance combustion, a ceramic burner throat ("quarl") extends the combustion chamber by two feet. Burner flow patterns, residence times, gas time/temperature histories and geometric relationships were representative of small-size burners in commercial furnaces.

Flame intensity through the rear 1 inch sight port was measured using an Ocean Optics, Inc. S2000 single fiber optic spectrometer. The spectrometer collected data along a line of sight passing by the centerline of the burner. The photo detector was sensitive over the wavelength range from 200 to 850 nm. Flame images were also obtained from a 4 inch open port located at the combustor rear access door, using a Lenox high-resolution camera/periscope.

Figure 4. Camera set-up at the combustion facility

A baseline test was performed for reference at the beginning of each test day. Reference conditions were: 1.45 Million Btu heat input, 80/20 secondary/tertiary air flow ratio and an air/fuel ratio corresponding to stoichiometric conditions (equivalence ratio, $\varphi = (A/F)_{stoic.}/(A/F)_{actual} = 1.0$).

A series of tests was performed at baseline heat input and secondary/tertiary air flow ratios for different air/fuel ratios (weight ratios) ranging from approximately 14.5 to 19.5 (φ =1 for a ratio of 17.1). This range of air/fuel ratios corresponds to a range of equivalence ratios from 0.9 to 1.2. Greater equivalences ratios represent fuel-rich conditions.

The range of excess O_2 corresponding to these equivalence ratios was from 0.0 to 2.2 percent. NO_x ranged from approximately 100 to 170 ppm_v. CO ranged from 100 to over 4,000 ppm_v for fuel-rich conditions. The centerline "quarl" gas temperature as indicated by the thermocouple varied from 2,800°F for fuel-lean conditions to approximately 3,100°F for fuel-rich conditions.

A key objective of the tests was to correlate flame characteristics (features[1]) with operating parameters and performance indices such as air/fuel ratio (flame stoichiometry), secondary/tertiary ratio (flame swirl), excess air (stack O_2), NO_x and CO emissions. Operating parameters, such as air and natural gas flow rates, stack O_2, NO_x, CO and CO_2 and "quarl" gas temperatures were measured directly or calculated from other plant instrumentation. Sample images are given in Figures 5. Figure 6 shows the result of feature analysis of images in Figure 5, confirming how easily these two conditions can be classified apart from their images.

It was found that NO_x, CO and gas temperatures decreased for increased swirl. A significant increase on NO_x emissions occurred at larger heat inputs (constant equivalence ratio and secondary/tertiary air flow ratio). The "quarl" gas temperatures were not greatly affected by changing the fuel heat input.

[1] Features are mathematical models representing certain flame characteristics.

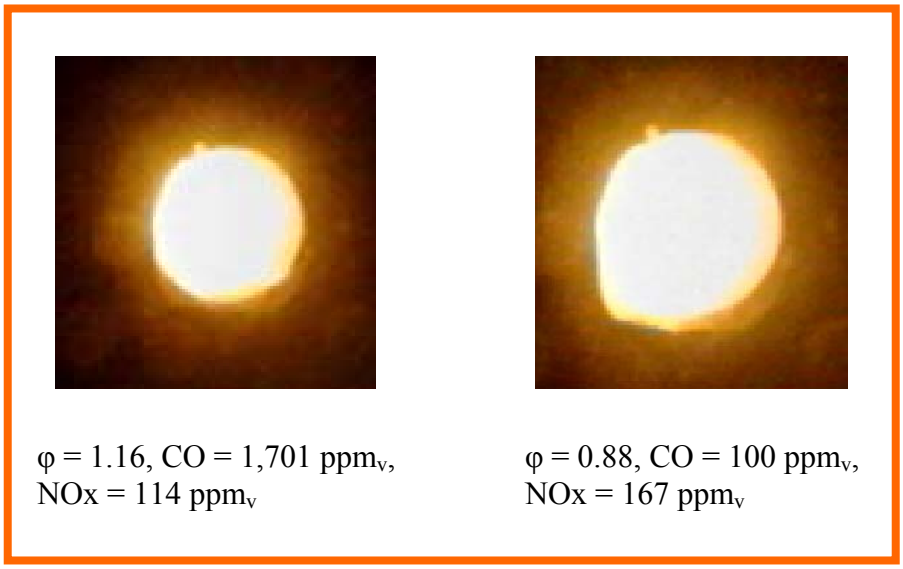

φ = 1.16, CO = 1,701 ppm_v, NOx = 114 ppm_v

φ = 0.88, CO = 100 ppm_v, NOx = 167 ppm_v

Figure 5. Sample images and their corresponding conditions

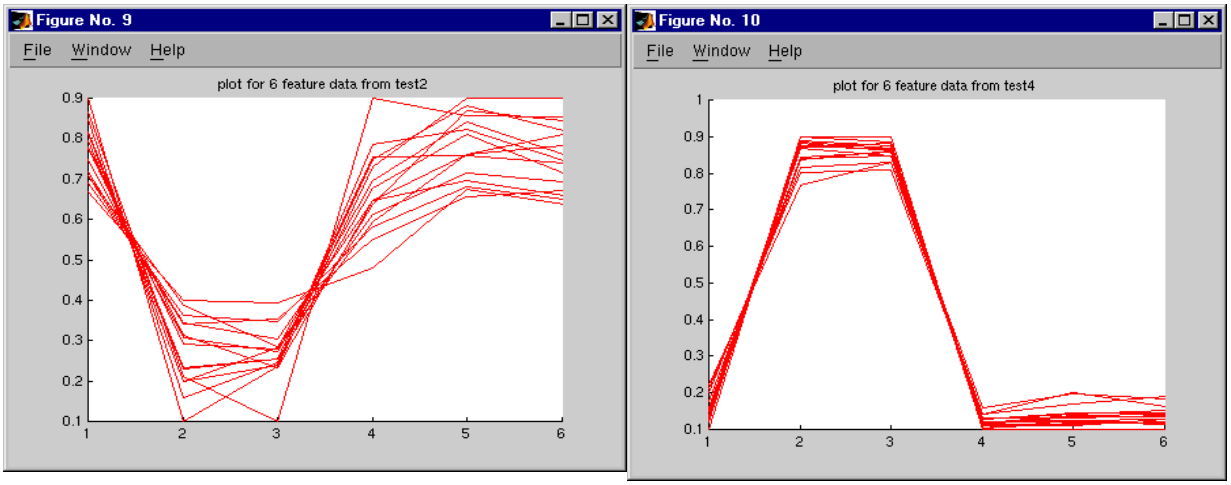

φ = 1.16, CO = 1,701 ppm_v, NOx = 114 ppm_v

φ = 0.88, CO = 100 ppm_v, NOx = 167 ppm_v

Figure 6. Plot of extracted features from images under two different conditions

SUMMARY OF ACCOMPLISHMENTS DURING FIRST YEAR OF PHASE II

The main activities during the first year of phase II as reported here were:

1. Design of experiments for furnace control integration
2. Spectrometer equipment upgrade for UV range and operation in harsh environment
3. Development of virtual temperature sensing
4. Macroscopic versus Microscopic time varying Flame Image Analysis
5. Assessment of Decision Tree versus Neural Network for image classification
6. Off-line control experimentation at pilot scale glass furnace

The data acquisition and analysis in Phase II were from three sources:

1) Various tests changing oxygen/fuel ratios and heat input at different furnace configurations as well as step and ramp-up tests. These tests were performed at the pilot scale single burner glass furnace in Rolla, Missouri.

2) Various tests including changing heat input in a double burner commercial glass furnace, Flat River Glass Company in Missouri.

3) Various tests by changing the fuel input to a particular burner and parametric tests at different oxidant/combustible ratios at both oxy fuel and air fuel commercial glass companies.

The report for the first year of phase II starts with a brief description of tests performed at the pilot scale test facility and experimental set-up used in Phase II. Then the accomplishments are described for four categories: 1) Spectral data analysis, 2) Virtual temperature sensing, 3) Flame image analysis using both single burner pilot scale facility as well as double burner commercial glass furnace, 4) Decision Tree versus Neural network for image classification, and 5) Control experimentations.

Tests & Control Experimentations at the Pilot Scale Glass Facility

The purpose of these tests was to obtain spectral data and flame images for oxy-fuel firing over a range of heat inputs and oxygen/fuel ratios. The experiments included rapid (step test) and slow (ramp test) change from fuel lean to fuel rich and fuel rich to fuel lean conditions, as well as, base line data collection at various oxygen/fuel ratios.

Although the goal of this project was to utilize images obtained from camera for image analysis, the role of spectroscopic data analysis using a spectrometer should not be undermined. The spectrometer was used in this project for the following objectives: 1) providing relationship between emission lines and various experiments (i.e, ramp and step tests) and flue gases such as NOx, 2) validating the image processing results through another established technique (i.e., spectroscopic data analysis), and 3) providing a one dimensional temperature measurement technique.

A total of 25 tests were performed in the first experiment on February 5 and 6, 2002 and 15 tests in the second experiment on March 16, 2002. The heat rate to the furnace was varied from approximately 80,000 to 165,000 Btu/hr. The oxygen/fuel ratio was varied from 1.8 to 2.4. Furthermore, separate tests were performed to obtain data on the response of the flame images and emission spectrum under combustion control step changes and under ramp-up conditions. Additionally, on April 9th 2002 several step and ramp-up experiments with longer duration were performed.

The spectrometer was upgraded in Phase II experimentation to improve its data acquisition capabilities. The new spectrometer is composed of two gratings running in parallel with a bifurcating fiber optics cable. The two gratings are sensitive over the 200-400 nm and 200-850 nm ranges, respectively. The 200-400 nm spectrometer allows detailed measurements of electronic-vibrational spectral activity of flame radicals, such as OH, CH and CN species, which can be used for indication of their relative concentrations. The two gratings overlap in the ultraviolet side of the spectrum, providing a way to check the validity of each other's readings. Spectral measurements at wavelengths covered by the 400-850 nm allow temperature calculations based on the blackbody emission from the flame. Additionally, the new spectrometric set-up was upgraded with a USB converter. The USB analog-to-digital converter increased the data transfer rate between the spectrometers and the data acquisition computer. This has improved the reliability of the system and allowed faster sampling rates at a wider range of operating conditions.

Furthermore, to install the spectrometer lens (and the attached fiber optics) inside the harsh environment of the furnace, a water/air-cooled probe case was designed and fabricated at a local machine shop as shown in Figure 7. The lens was mounted in the water/air-cooled probe and positioned at the rear end of the furnace (see Figure 2-c) focusing on the combustion zone of the flame under different operating conditions. Spectral data were collected over the entire wavelength ranges and for specific wavelength bands centered on the 290 and 310 emission lines for the OH radical and for peaks around 345 nm. Figure 8 shows a sample plot of both the UV and the VI spectrum collected on March 16, 2002. Figure 9 shows a characteristic spectral distribution from a point within the flame at three different oxygen/fuel ratios in the spectral range from ultraviolet to approximately visible green. The traces represent average data over the data collection time. Fuel leaner conditions resulted in an increase in the peak strength of the OH radical as shown in Figure 9.

Figure 7. The water/air-cooled probe case system for the spectrometer

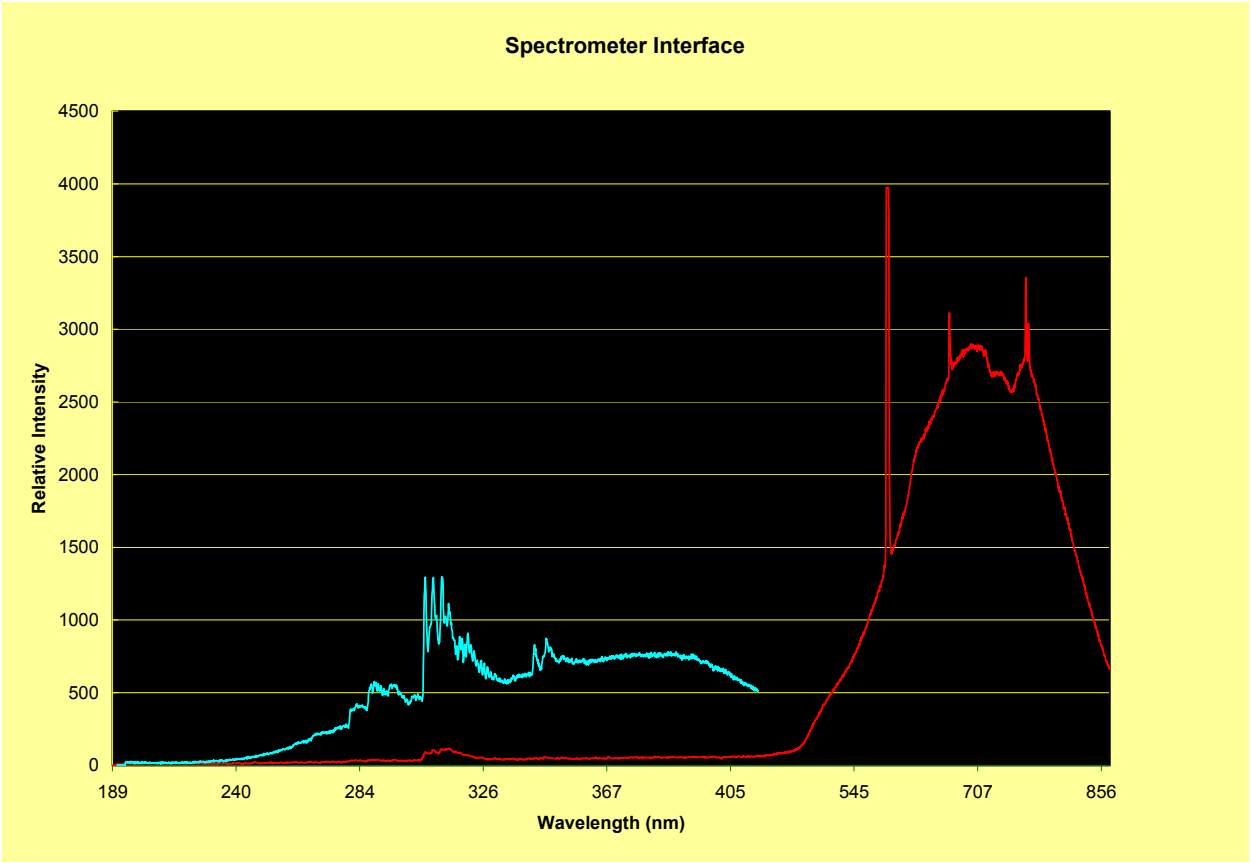

Figure 8. A sample plot of both UV and VI spectrum

The variations of the OH spectral band were studied in detail because they showed good response and sensitivity under the various experimental conditions. Data presented correspond to the overall OH peak strength taken as the average of the multiple peaks in the electronic-vibrational band around 310 nm. A statistical analysis of the data was performed to determine the magnitude of the random fluctuation of the spectral distribution due to the flame flickering. Figure 10 indicates that in the bands of interest, the relative fluctuation is less than 5 percent of the average value.

Figure 11 shows the OH radical spectral intensity (around the 310 nm spectral band) as a function of burner oxygen/fuel ratio. Again, as expected, fuel leaner conditions resulted in an increase in the peak strength of the OH radical. Figure 12 shows a plot of the OH radical peak intensity as a function of natural gas flow rate.

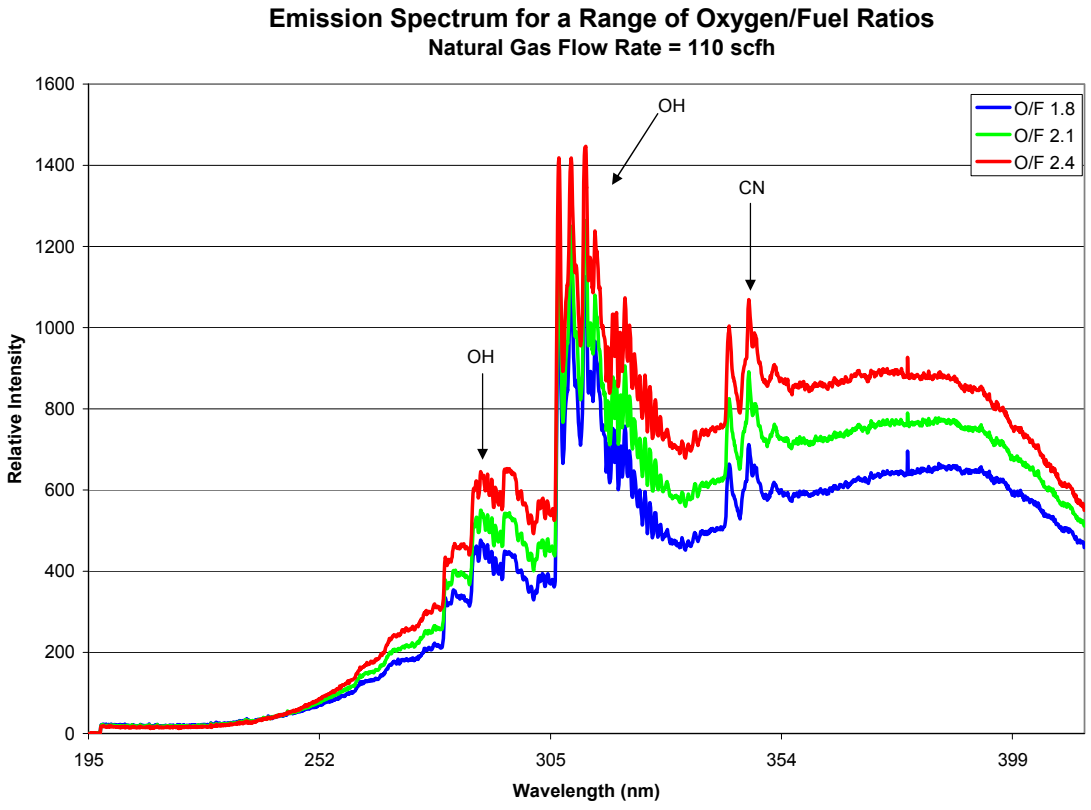

Figure 9. Emission spectrum in the 200-400 nm range

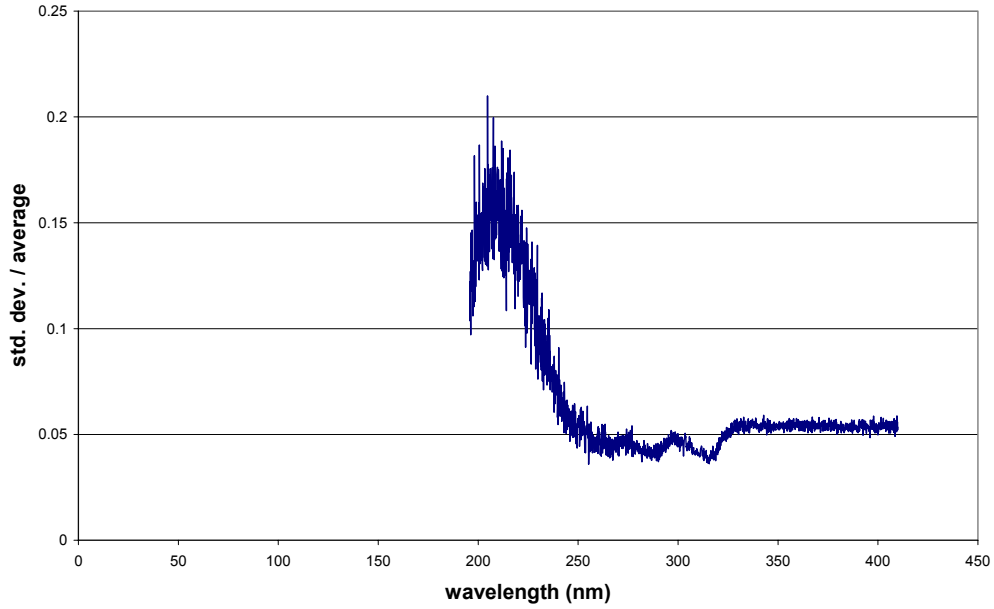

Figure 10. Relative signal fluctuation as ratio of standard deviation over the average value

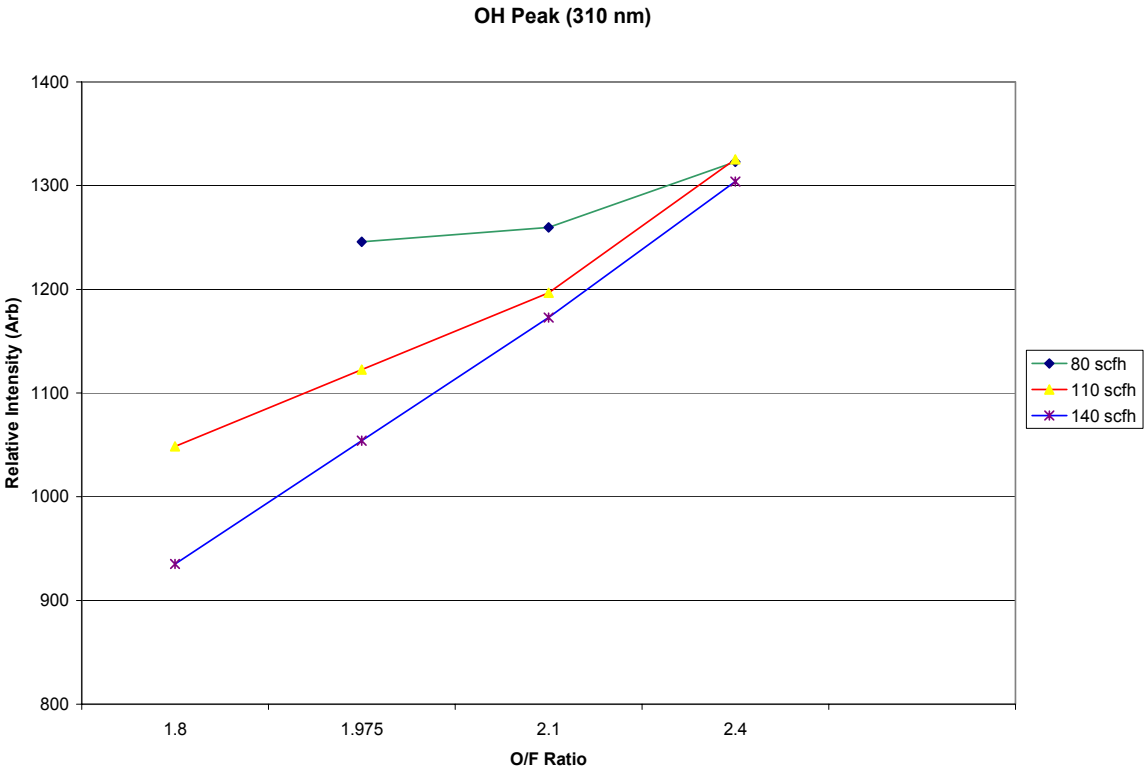

Figure 11. OH radical spectrum intensity variation with O/F ratio

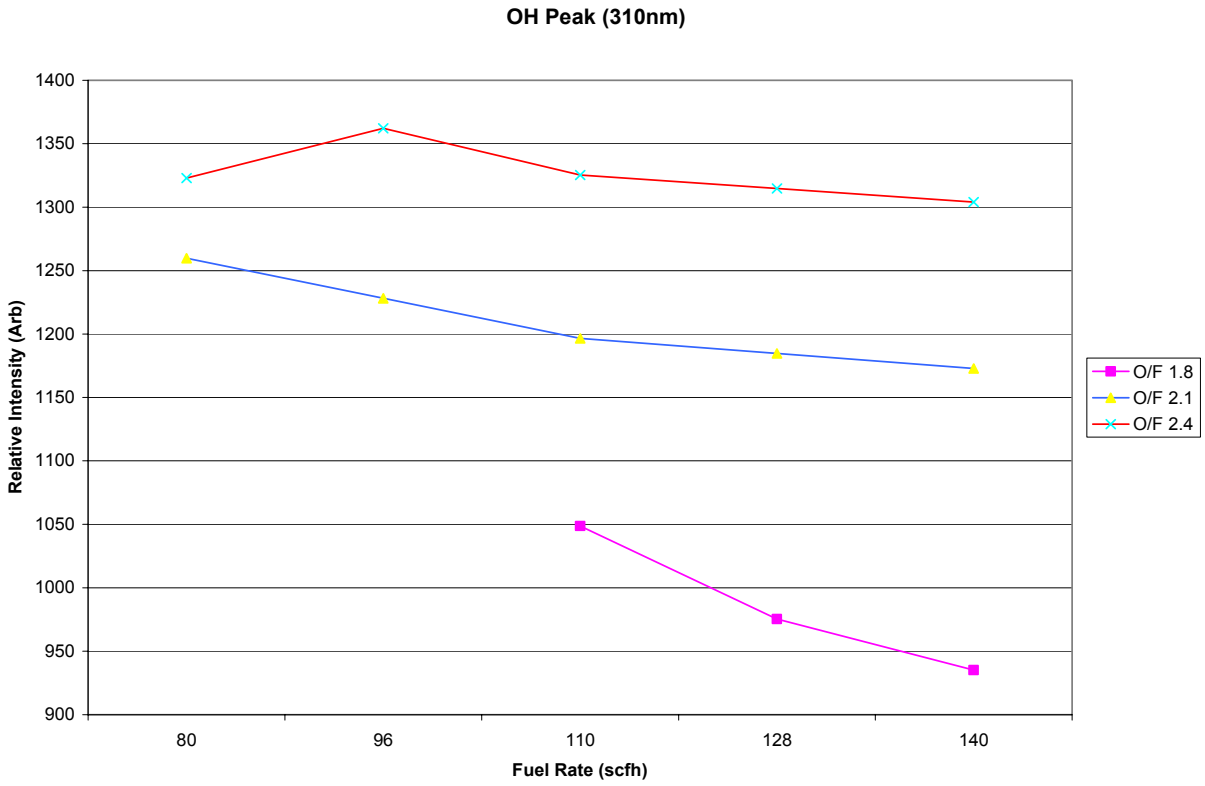

Figure 12. OH radical peak intensity as a function of natural gas flow rate

Virtual Temperature Sensing

Temperature calculations were performed to provide a reference furnace temperature based on the electromagnetic radiation of the flame. A blackbody reference was used to correct for wavelength-dependent losses in the spectrometer and fiber optic cable (the output from the 200-850 grating was used). A 3100 K tungsten Halogen lamp provided the reference blackbody spectrum.

Virtual temperature sensing is accomplished by two different methods, 1) best fit approach, and 2) intensity ratio approach, as described below.

Spectrometer Efficiency Calculation

Figure 13 shows the expected emission at 3100 K based on Planck's law and the measured spectral distribution. The decrease in the recorded relative intensity is due to the efficiency of the combined grating and fiber optic set-up wavelength range. This information was used to estimate the relative optical efficiency of the spectrometer system for temperature calculations as shown in Figure 14.

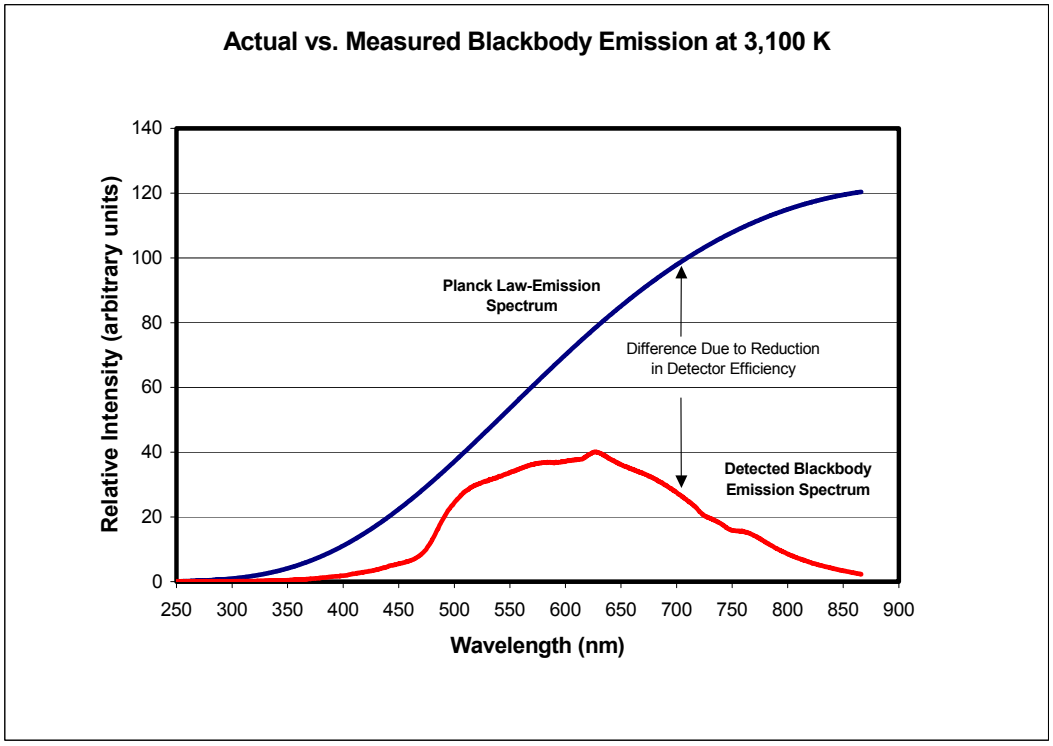

Figure 13. Plot of measured and blackbody emission at 3100 K

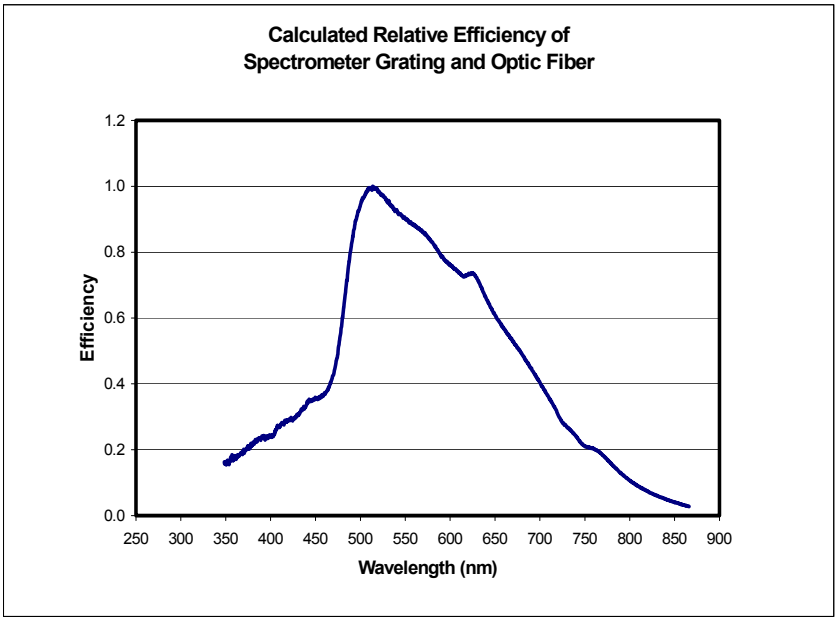

Figure 14. Plot of the calculated spectrometer efficiency as a function of wavelength

Method 1: Best Fit Approach

This approach is based on the assumption that the measured spectrum is a composite of two blackbody profiles at different temperatures T_1 and T_2 plus a constant background. Temperature T_1 represents the hot combustion gases and T_2 the wall temperature as represented in the following equation:

$$I_{bb,meas}(\lambda) = A\,\eta_{spec}\left(E_{\lambda,bb}(\lambda,T_1) + E_{\lambda,bb}(\lambda,T_2)\right)$$

$$E_{\lambda,bb} = \frac{2\pi hc^2}{\lambda^5\left(e^{\frac{hc}{\lambda\kappa T}} - 1\right)}$$

η_{spec} is the calculated efficiency of the spectrometer grating and optical cable. The parameter A is a correction factor.

Where,

I: Intensity
λ: Wavelength
T: Temperature
h: Planck's constant
k: Boltzmann constant
c: Speed of light

The experimental blackbody temperature of the various flames was calculated using a best-fit approach whereby the measured spectrum was approximated by a theoretical blackbody spectral distribution based on temperature contributions from the flame and furnace wall. This approach provides an integral fit over the entire wavelength range and includes the necessary correction to account for the optical efficiency of the system.

Figure 15 shows the agreement between the measured and best-fit spectra for the case where the burner was turned off at the end of the experiment (i.e., no flame) and a set of spectrometer readings was taken immediately after. Figure 16 shows the comparison between the spectral data and best-fit trace for a test run corresponding to an oxygen/fuel ratio of 2.1. In these traces, the thermal radiation in the analyzed spectral range appears as background radiation, which increases slowly with increasing wavelength (Planck radiation). Superimposed on the spectral distribution are the individual spectral lines that are characteristics of intermediate and end products of combustion and based on the chemiluminescence phenomenon. The spectral line around 590 nm corresponds to sodium from the glass furnace.

Figure 17 shows the experimental blackbody temperature as a function of the oxygen/fuel ratio for various data. The variation of the calculated temperature with oxygen/fuel ratio exhibits the expected trend, decreasing as the mixture became fuel leaner.

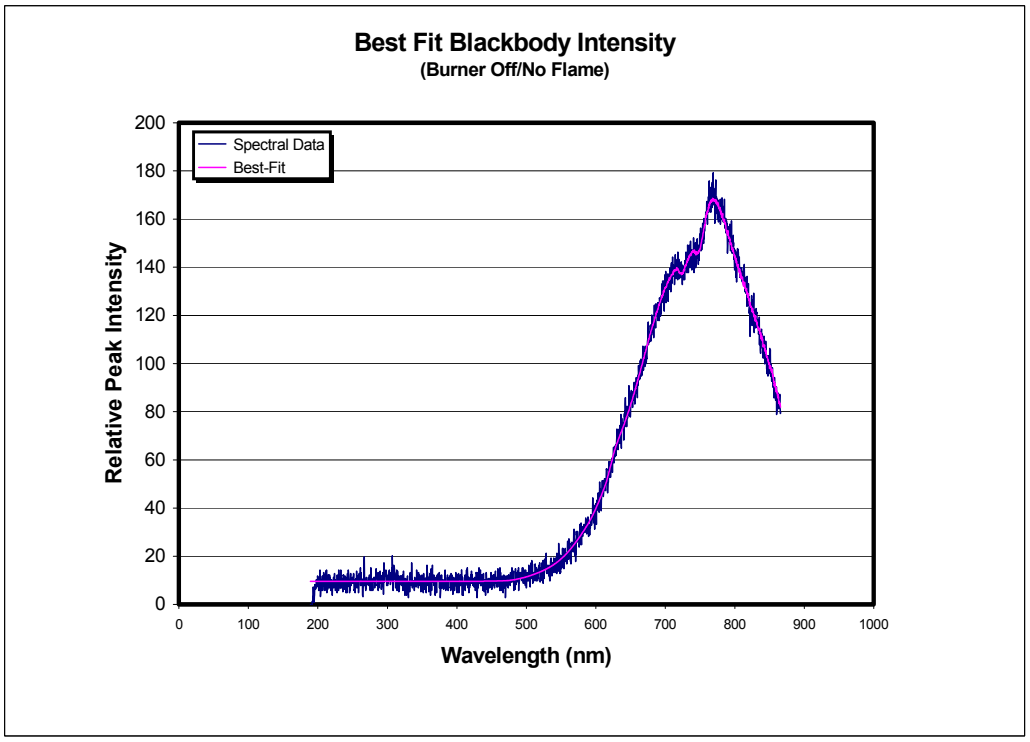

Figure 15. Plot of measured and best-fit spectra with no flame condition

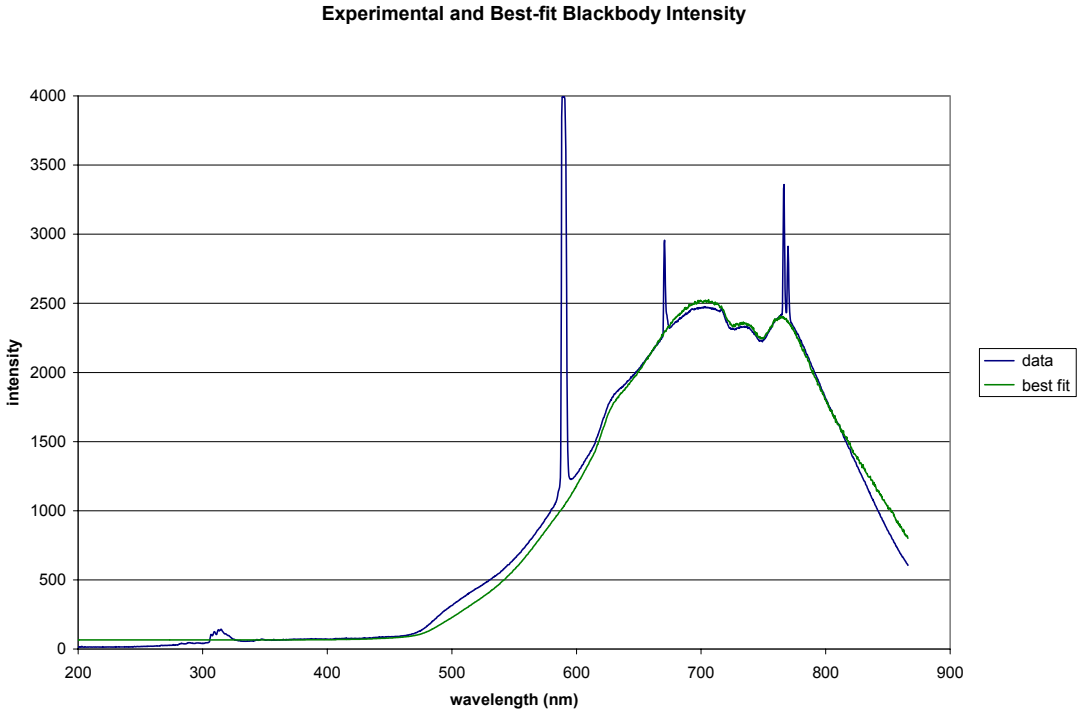

Figure 16. Spectral data and best-fit blackbody trace for VIS region

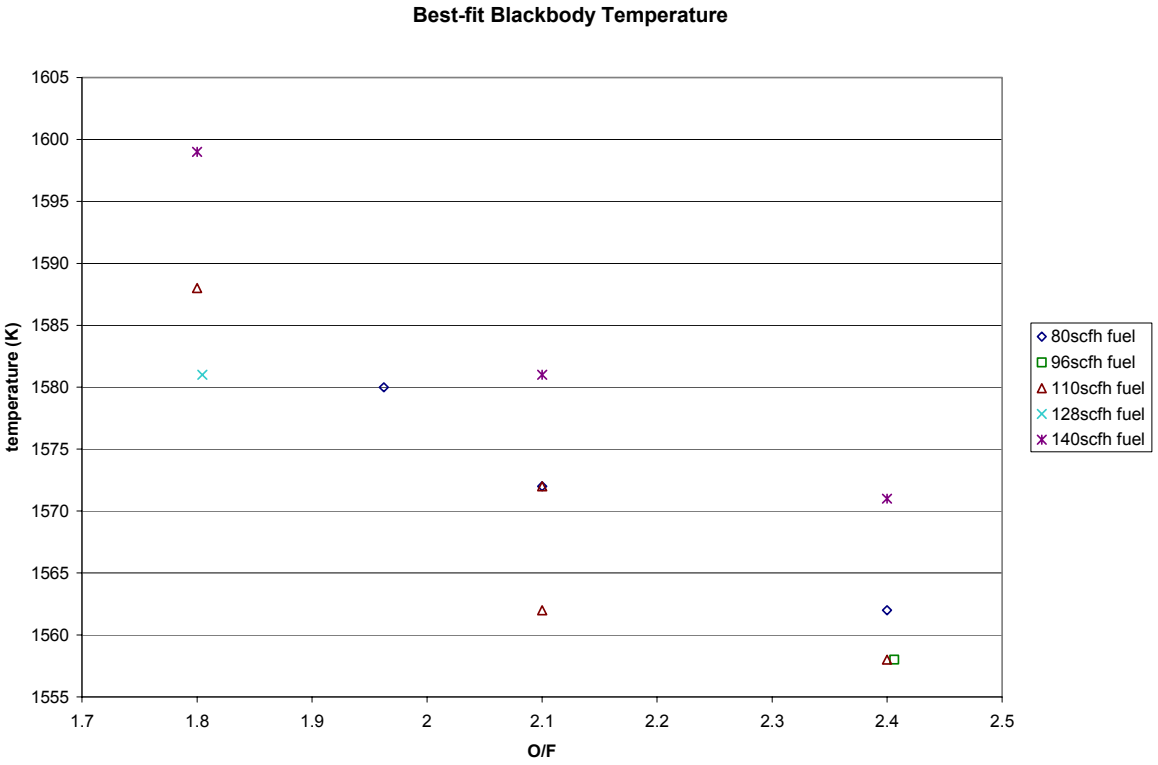

Figure 17. Plot of calculated temperature as a function of the oxygen/fuel ratio

Method 2: Intensity Ratio Approach

This approach is based on ratio of intensities of a pair of wavelength along a selected spectrum as described below.

The Tungsten Halogen lamp is used as a reference spectrum (3100 K) and the spectrum is being analyzed as black body radiation. Since the units of the intensity are unknown, the ratios of the intensities at two different wavelengths are compared to the ratio of the blackbody radiation equation at those two wavelengths and solved for the temperature according to the following equation:

$$I_1\lambda_1^5/I_2\lambda_2^5 = (e^{(hc/\lambda_2 kT)} - 1) / (e^{(hc/\lambda_1 kT)} - 1)$$

Where,

I: Intensity
λ: Wavelength
T: Temperature
h: Planck's constant
k: Boltzmann constant
c: Speed of light

Table 1 shows the calculated temperature by this method for various NG and O/F ratios.

Table 1: Calculated temperatures for various NG and O/F ratios

Temp (K)	NG (scfh)	O2 (scfh)	O/F
1726	110	231	2.1
1701	80	158	1.975
1722	110	198	1.8
1803	140	252	1.8
1707	80	168	2.1
1762	110	231	2.1
1749	140	294	2.1
1684	80	192	2.4
1727	110	264	2.4
1824	140	335	2.4
1699	96	231	2.4
1736	110	231	2.1
1757	128	231	1.8

Flame Images from the Pilot scale Glass Furnace

Camera images of burner flame using oxy-fuel with various oxygen/fuel (O/F) ratios were collected at the pilot scale glass furnace. Figure 18 shows three sample flame images for O/F ratios 2.4, 2.1, and 1.8 generated by keeping oxygen flow rate at 231 scfh and varying the natural gas flow rate from 96 to 128 scfh. Thresholding technique is used for edge detection of each flame image, then the features are extracted. Feasibility study of Phase I showed that the dynamic behavior of the flame image pattern does not interfere with the uniqueness of each image pattern. In Phase II a new approach was elected and referred to as "macroscopic" approach in analyzing the images. In this approach, each characteristic feature is averaged over the entire 30 frames obtained from each second of video clip and a plot of ten seconds is provided for comparison of various tests. Furthermore, in Phase II more elaborate feature sets were generated and more images tested. Figure 19 shows the plot of features extracted for ten seconds image data collected at 1.8 (fuel rich), 2.1 (stoichiometry condition), and 2.4 (fuel lean) O/F ratios. Figure 19 clearly shows that macroscopic feature patterns are easily separable. The results confirm that the proposed methodology will be successful in recognizing each operation apart through pattern recognition of the corresponding flame patterns generated from the unique features of the associated flame images.

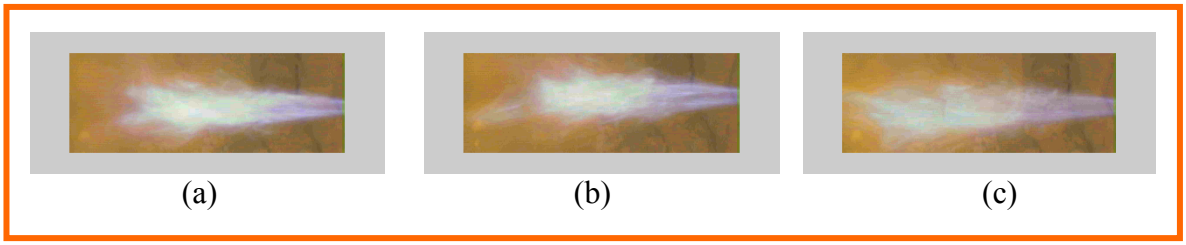

Figure 18. Flame images at (a) 2.4 O/F ratio, (b) 2.1 O/F ratio, c) 1.8 O/F ratio

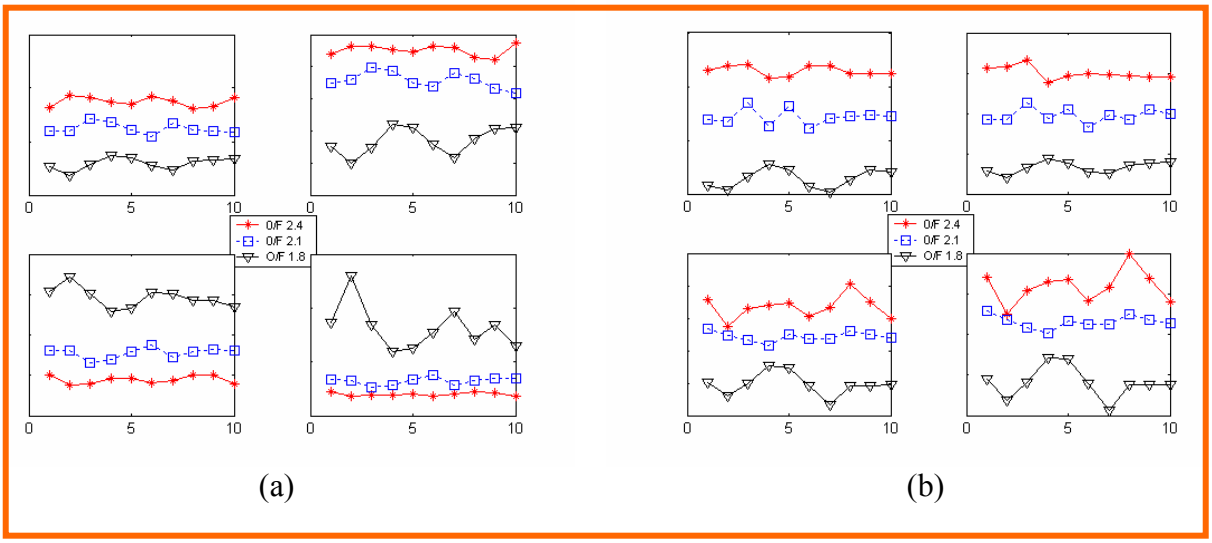

Figure 19. Plots of two groups of features (a & b) for 10 seconds macroscopic behavior of the flame at various O/F ratios

Commercial Glass Furnace (two-burner)

The selected commercial glass company operated two continuous furnaces, both producing soda-lime silicate container glass. Data acquisition took place on March 16, 2001.

Both furnaces are end-fired with regenerative heat recovery. The nominal production throughput of each furnace is approximately 105-110 U.S. tons per day.

Spectrometer data and camera images were collected. Figure 20 shows a sample of side and back view images.

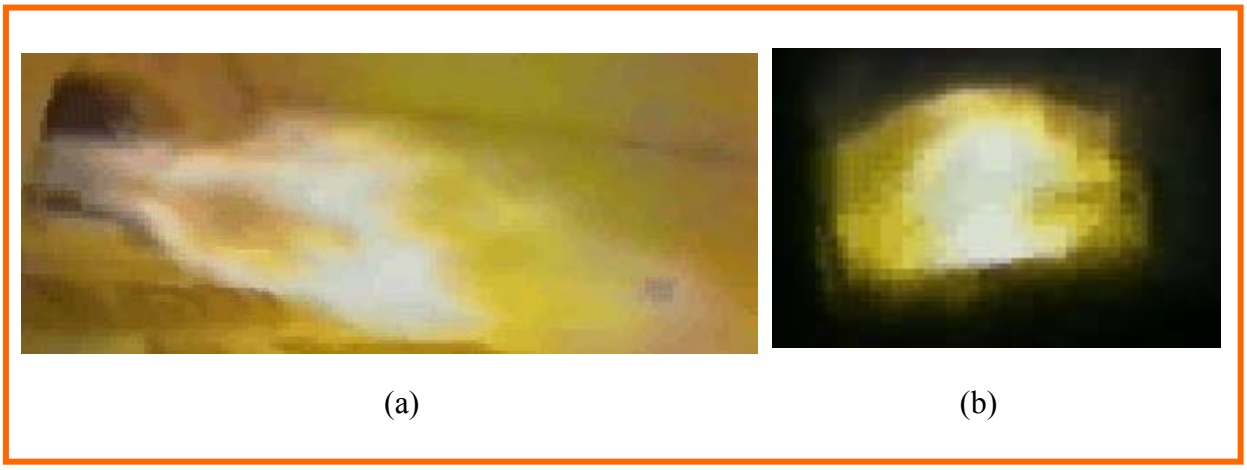

(a) (b)

Figure 20. Sample images from commercial Glass furnace: a) side view, and b) back view

Figure 21 shows the result of macroscopic approach using eight seconds of data from side view for two firing rate conditions that are one KW (3412 Btu/hr) apart in the rate of heat input. The "full 01" data represent lower firing rate. There are two sets of feature patterns and eight in total. This result confirms that direct extension of the macroscopic approach to a 2-burner flame images from commercial furnace is just as successful as the pilot scale flame for monitoring flame condition.

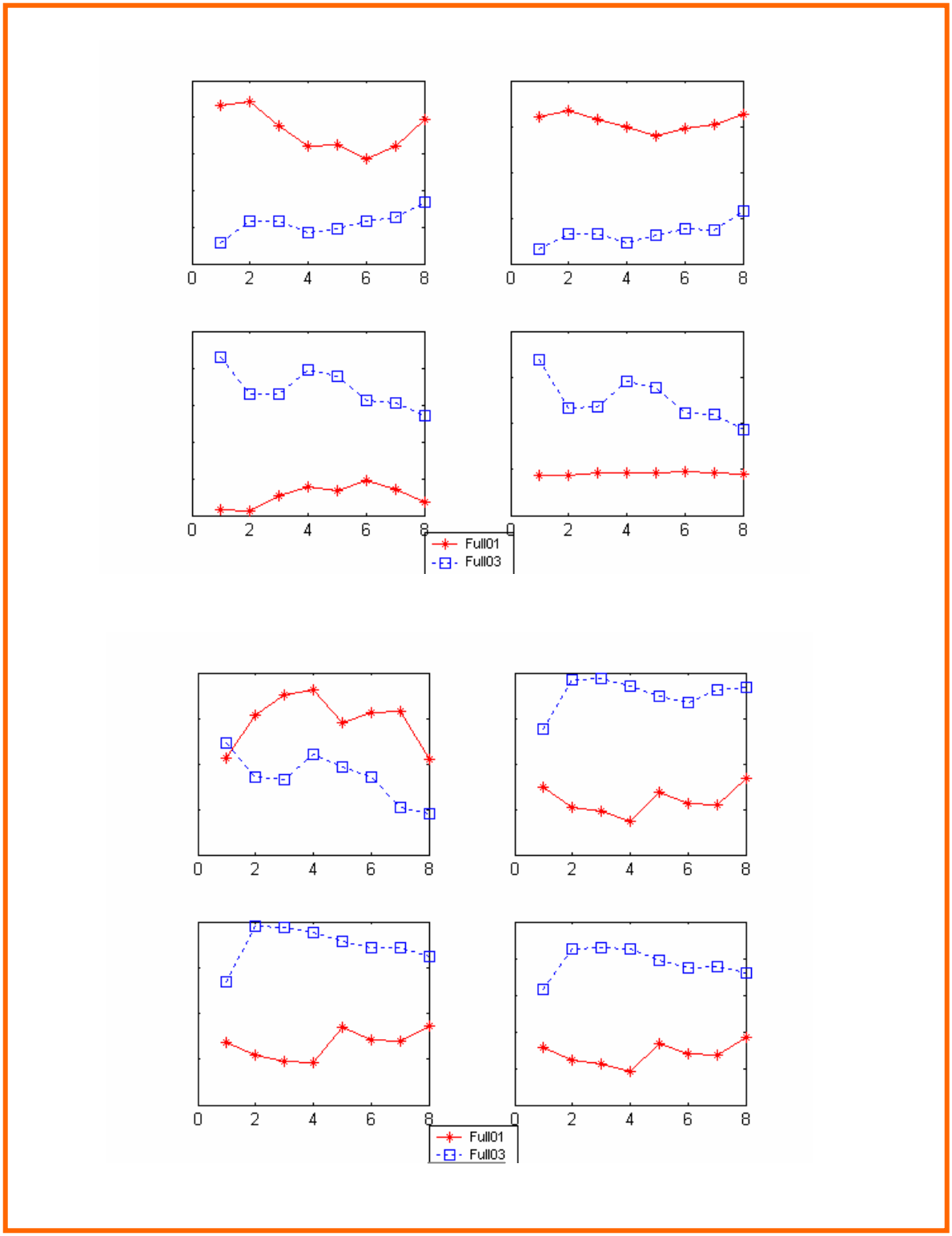

Figure 21. Plot of features for two input heat rate conditions

Assessment of Decision Tree versus Neural Network

Data mining refers to extracting or "mining" knowledge from large amounts of data. Decision Tree (DT) is a data mining technique. Classification analysis in Phase I was performed using Adaptive Resonance Theory (ART) family of neural networks. In Phase II, DT technique was examined for classification purpose. Then, a comparison of image classification performance of DT and Backpropagation (BP) neural network was carried out. Data from three operation conditions at pilot scale glass furnace were used for this analysis. The flowchart of the approach is shown below:

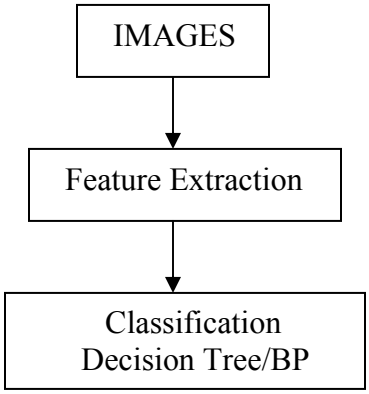

Decision tree uses gain criterion, BP is trained using Levenberg-Marquardt backpropagation by supervised training. Decision Tree focuses on information of the data set and gives the features that are critical to identify the classes, while BP simulates the neuron.

DECISION TREE

A Decision Tree is an arrangement of tests that prescribes an appropriate test at every step in an analysis. Entropy[2], a measure from information theory, characterizes the purity, or homogeneity, of an arbitrary collection of examples. DT algorithm is based on minimizing the average entropy by calculating the average entropy of each test attribute and choosing the one with the lowest degree of entropy.

More specifically, decision trees classify instances by sorting them down the tree from the root node to some leaf node, which provides the classification of the instance. Each node in the tree specifies a test of some attribute of the instance, and each branch descending from that node corresponds to one of the possible values for this attribute.

[2] Entropy in DT algorithm differs from the common entropy used in thermodynamics

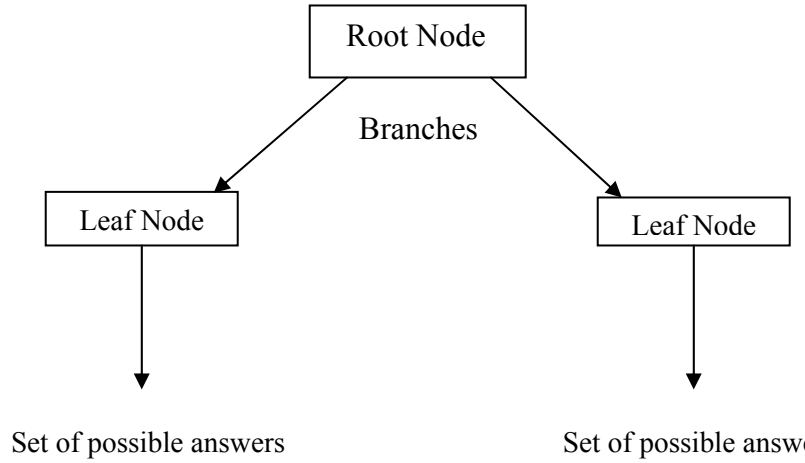

- Each branch carries a particular test results subset to another node.
- Each nonleaf node is connected to a test that splits its set of possible answers into subsets corresponding to different test results.
- Each node is connected to a set of possible answers.

NEURAL NETWORK

Neural net used for this comparison is a backpropagation net with one hidden layer. Different learning rate results in different convergence speed. Learning rate of 0.1 was selected which provided a good speed (no more than 30 epochs).

Conclusion: It was concluded that although both methods are comparable in performance, one tends to prefer DT for two main reasons: 1) Decision Tree may select features that are critical to identify the classes. This may help to choose the appropriate features among all presented features which are relevant to a specific classification, and 2) extra features that are not good representation for a particular classification would not confuse the DT and will not impact its performance, they would just be set aside in the entropy process, an inherent feature of DT algorithm.

Control Experimentations

Several experiments were performed to determine the dynamic response of the spectral signal and the flame image features to changes to the combustion control system. The spectral signals are characterized by the 310 nm spectral line for the OH radical and the 345 nm spectral line. For these tests, changes were made to the natural gas flow rate while keeping the oxygen control valve unchanged (or changing oxygen flow rate while keeping natural gas unchanged) resulting in oxygen/fuel ratio in the range between 1.8 and 2.4. Figure 22 shows the 345 nm peak data versus time as well as the measured O/F ratio and the intended O/F ratio from 1.8 to 2.4. For the ramp-up condition, changes to the control valve were made on a two-second interval.

Figure 23 shows two plots, one is the actual 310 nm peak data versus time, as well as, the O/F ratio, and the second plot shows the same 310 nm peak data after applying moving average processing to these data. This process helps to better visualize the OH radical peak following the ramp with a time shift caused by the moving average process.

Figure 24 shows similar plots for a step experiment showing the behavior of both 310 nm peak and 345 nm peak as a function of time.

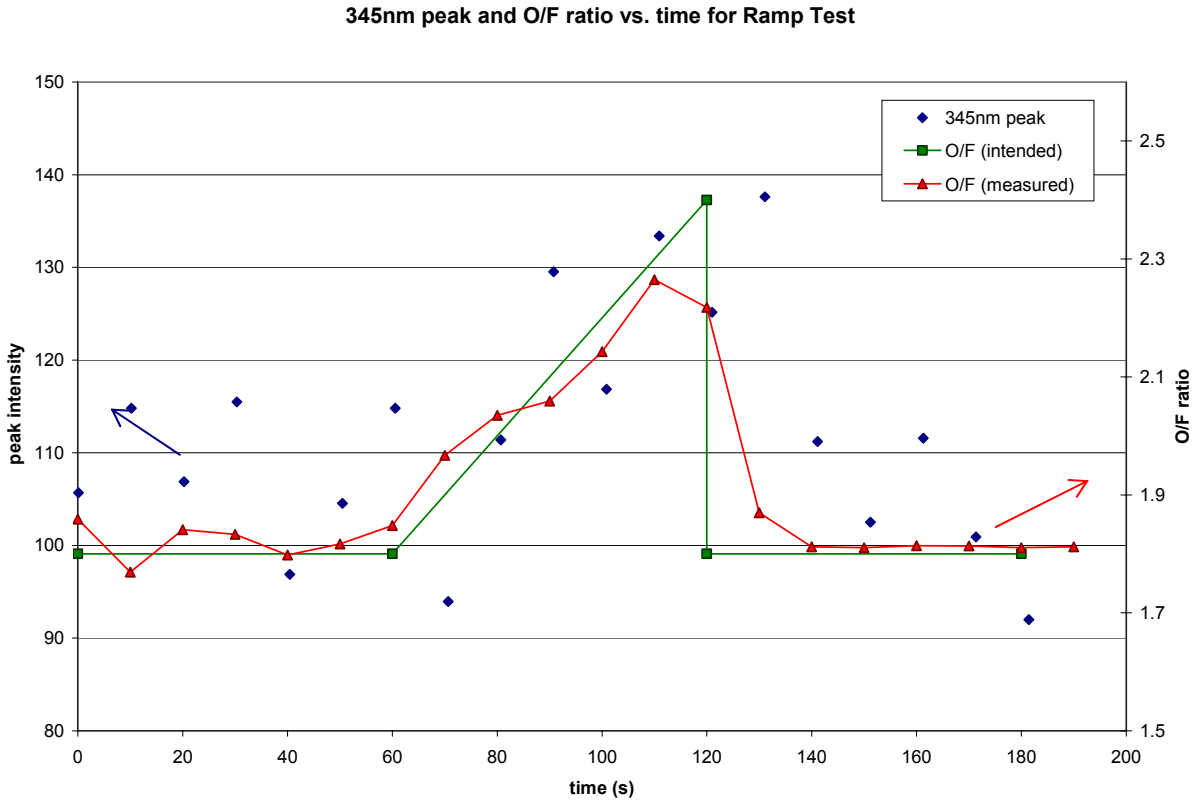

Figure 22. Plot of 345 nm spectral line peak values versus time for a ramp up experiment

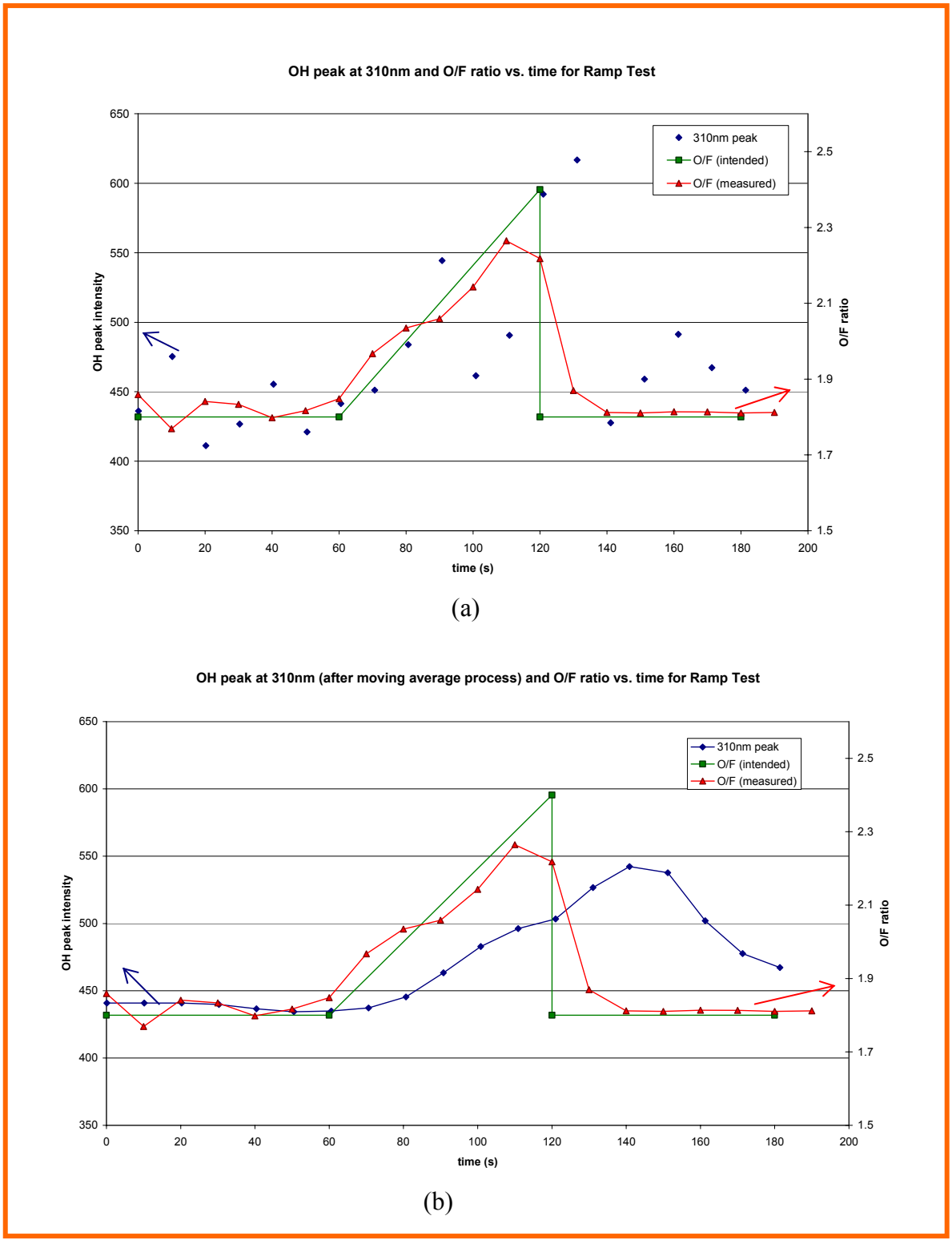

Figure 23. Plot of OH radical at 310 nm versus time for a ramp up experiment, (a) actual OH peak, (b) moving average values of OH peak.

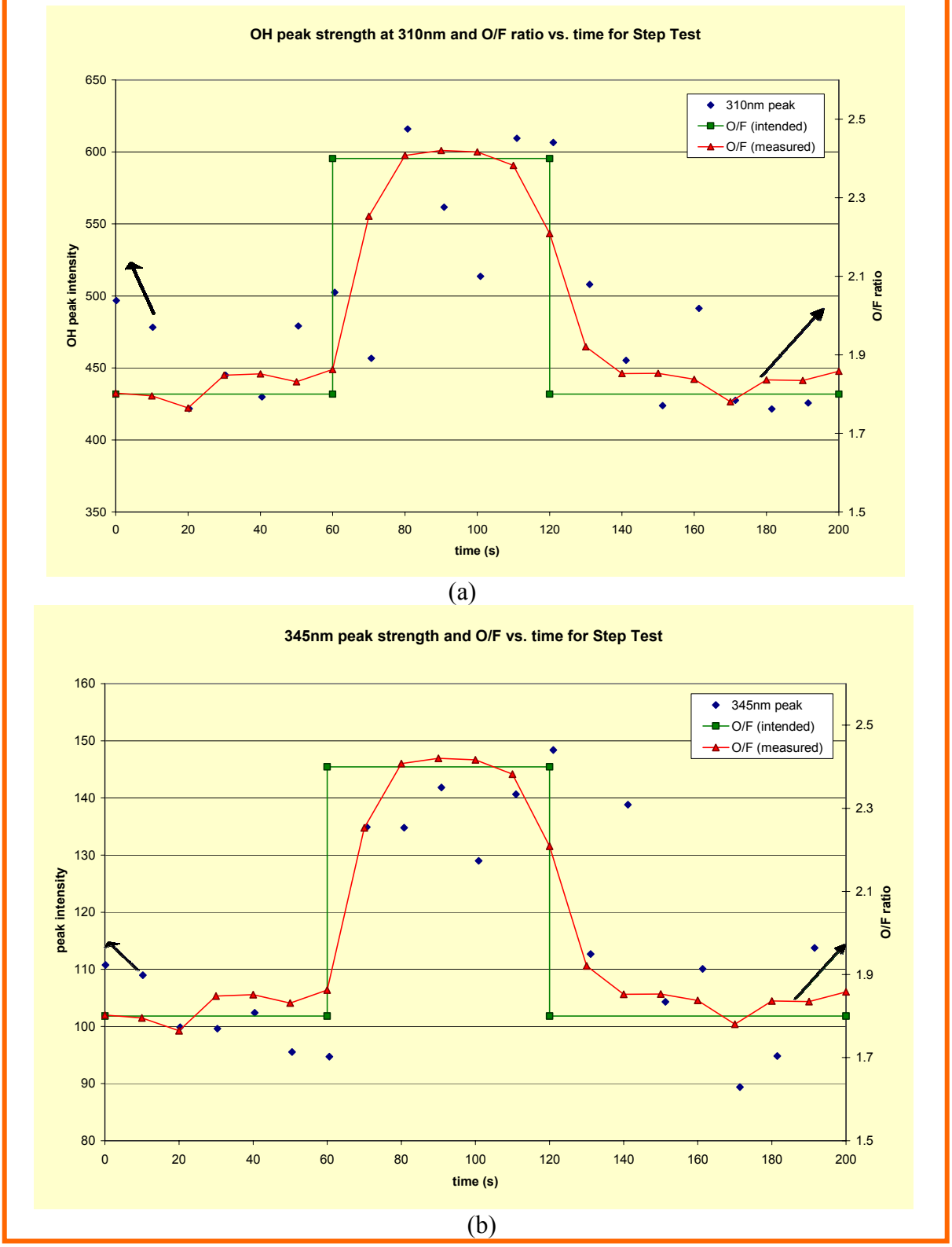

Figure 24. Plot of OH peak emission at 310 nm (a) and 345 nm (b) versus time for a step experiment

Figure 25 shows the plot of a sample image feature generated from 30 second image data of the step-down experiment followed by ten second (data points from 30 to 40 in the plot) feature data of the step-up experiment. Step-down experiment was generated by keeping the natural gas at 110 Scfh and changing oxygen flow rate from 264 to 198 Scfh in a stepwise fashion as shown in Figure 25. In the step-down experiment, it was observed that the time lag between the initiation of the reduction of oxygen until reaching its final value was six seconds. Figure 25 also shows how closely the feature follows the step-down change within the same 6 second time lag as the oxygen time lag. This is an important factor for control application.

The response to the ramp-up experiment is shown in Figure 26. This figure is a screen picture of a control simulation showing the behavior of one image feature in response to a ramp-up experiment. The ramp-up condition was generated by keeping the oxygen flow rate at 231 Scfh and reducing the natural gas (NG) flow rate from 126 scfh to 96 scfh over one minute time at a rate of two-second interval resulting in increased O/F ratio. Figure 26 shows how closely the feature is following the NG change.

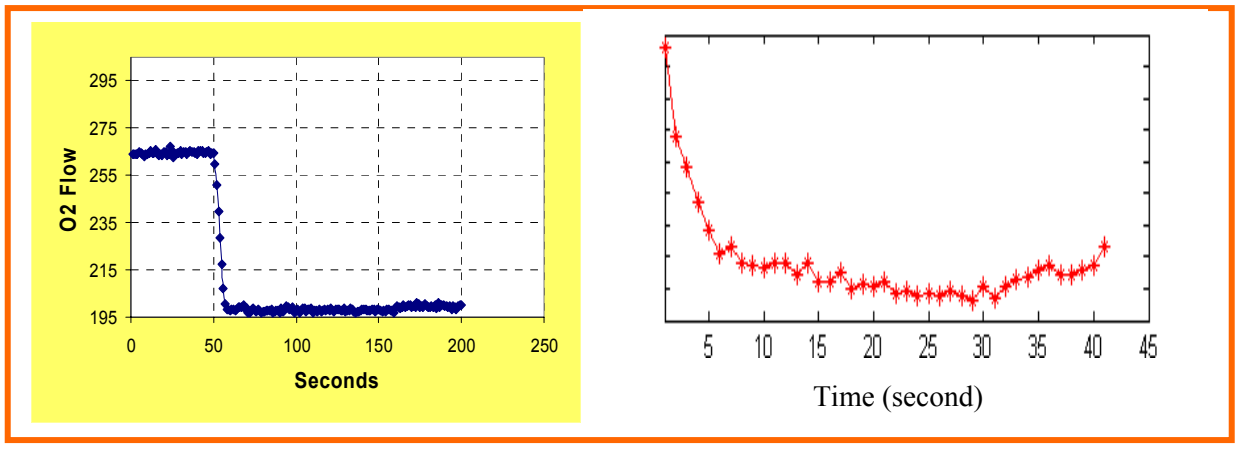

Figure 25. Plot of a stepwise oxygen reduction (left) and one feature behavior following this step change (right)

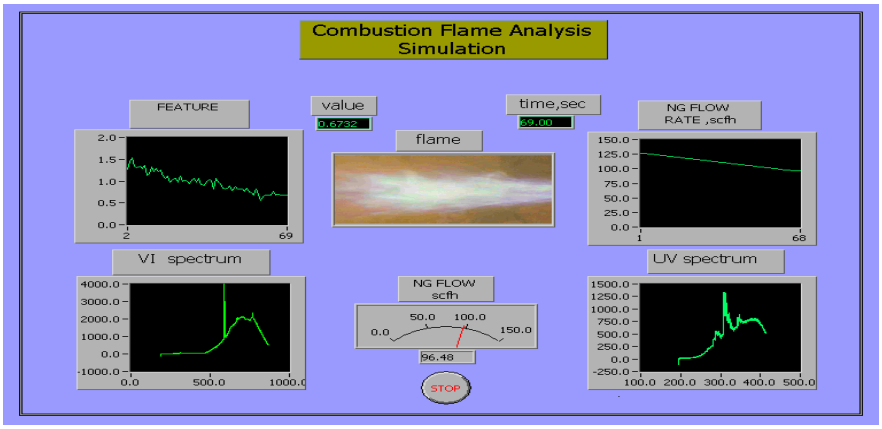

Figure 26. Screen picture of Labview control simulation

SUMMARY OF ACCOMPLISHMENTS DURING THE SECOND YEAR OF PHASE II

The main activities during the second year of phase II as reported here were:

- Verification of the technique for multi-burner (more than 2-burner) commercial glass furnace for both oxy fuel and air fuel furnaces
- Upgrading the spectrometer to near IR region
- Data acquisition from a selected commercial furnace for prototype development
- Prototype design
- Designing the Graphical User Interface (GUI) for multi-burner commercial glass furnace

The report for the second year of phase II starts with the experiments and results from an oxy/fuel multiburner commercial glass furnace followed by similar activities in an air/fuel multiburner glass furnace. Then a sample shot of the Graphical User Interface design is presented.

OXY/FUEL COMERCIAL GLASS FURNACE

The oxy/fuel commercial furnace was a Fiberglass manufacturing furnace rated at 13 Million Btu/hr. Figure 27 shows the camera set-up and a sample of the flame image at this furnace, where, each port housing two burners was individually controlled for its O/F ratio.

Figure 27. Camera set-up and a sample flame

On May 6-8, 2002, a series of tests were performed to determine the dynamic response of the spectral signal and the flame image features to changes to the combustion control system. On these tests, a pair of burners was targeted in terms of changing their oxygen/fuel ratio and heat input. Two series of eight tests were performed at 100% and 75% heat input. For each series of tests, the oxygen/fuel ratio was moved from 1.8 to 2.4. Additionally, data were collected on the response of the flame images and electromagnetic spectrum under combustion control ramp-up/ramp-down conditions. Flue gas excess O_2 and emission data (CO and NO_x) measurements are not available on this furnace on a continuous basis. A portable analyzer was mounted at the stack to obtain exhaust gas composition for each test. The impact of optimum combustion on NO_x reduction was measured using spectroscopic data and NO_x data from the flue gas analyzer. Figure 28 shows the set-up for Flue gas and Spectrometer at this furnace. Figures 29 and 30 show variations of OH (at 310 nm) and excess oxygen with O/F ratio respectively. Figure 31 shows relative NOx emission behavior with OH changes at two different heat input.

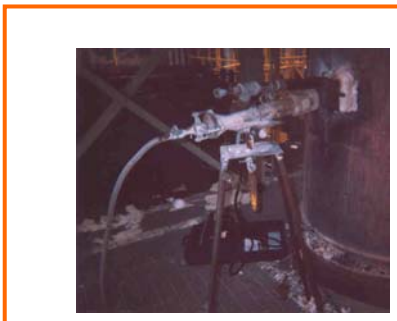

Flue gas sampling set-up

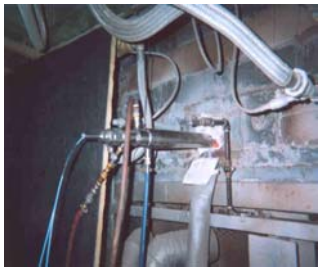

Spectrometer set-up

Figure 28. Mounting set-up for flue gas and spectrometer

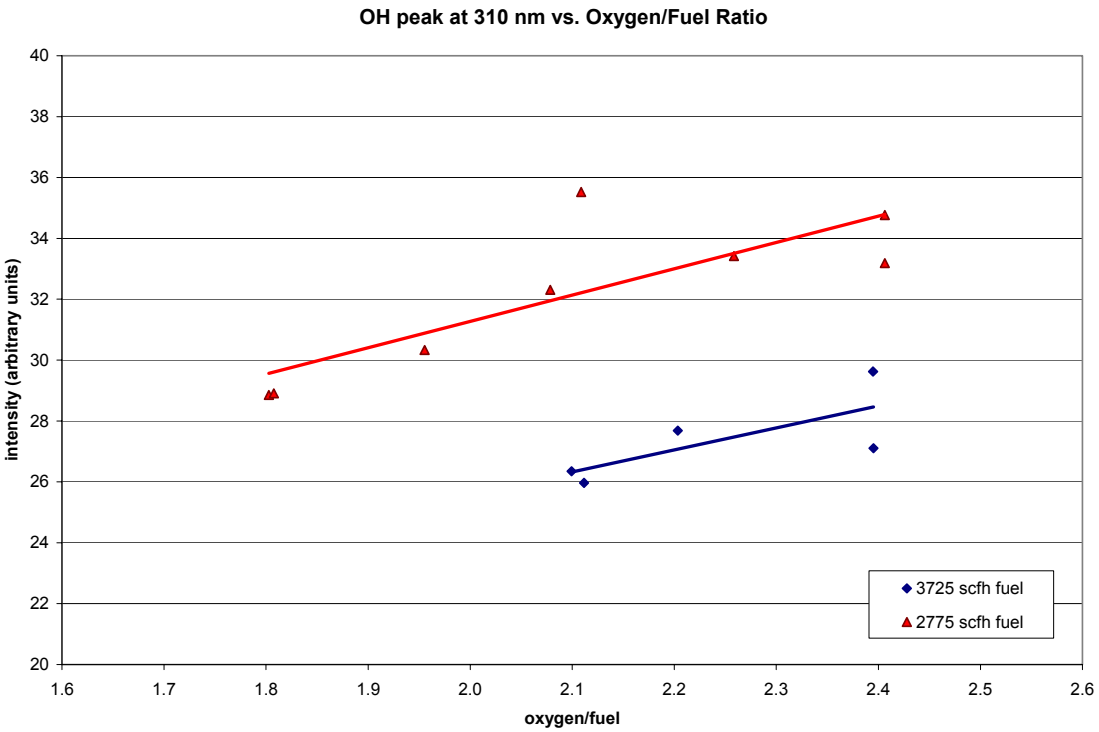

Figure 29. Variation of the OH with O/F ratio at two different heat inputs

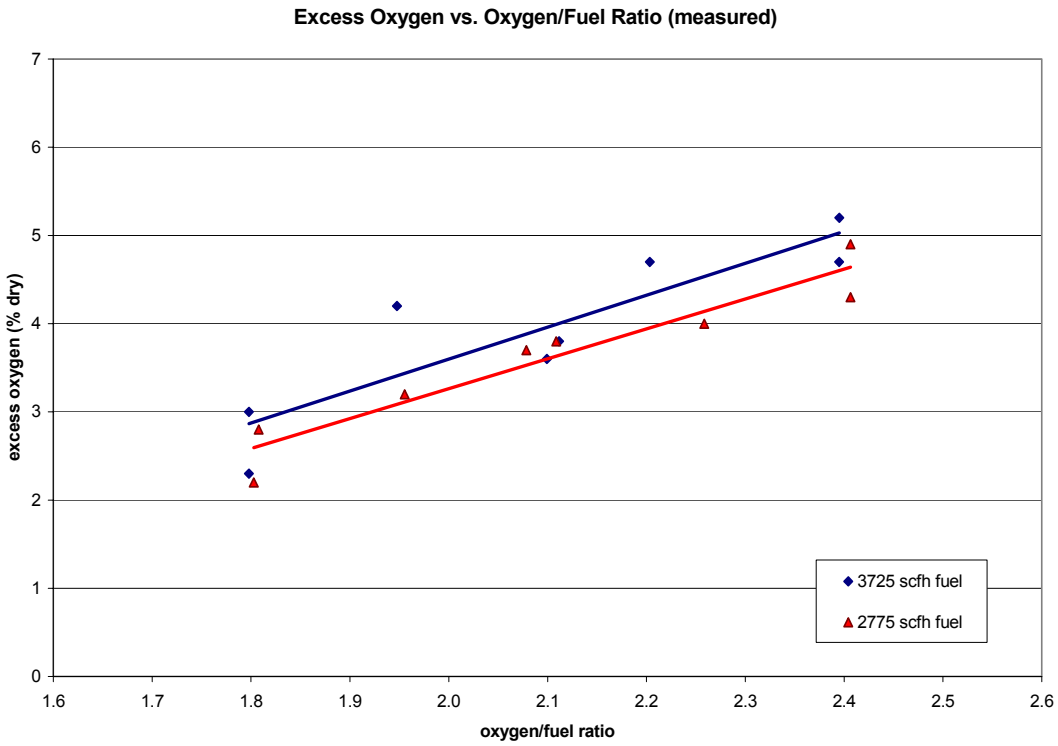

Figure 30. Variation of the excess oxygen with O/F ratio at two different heat input

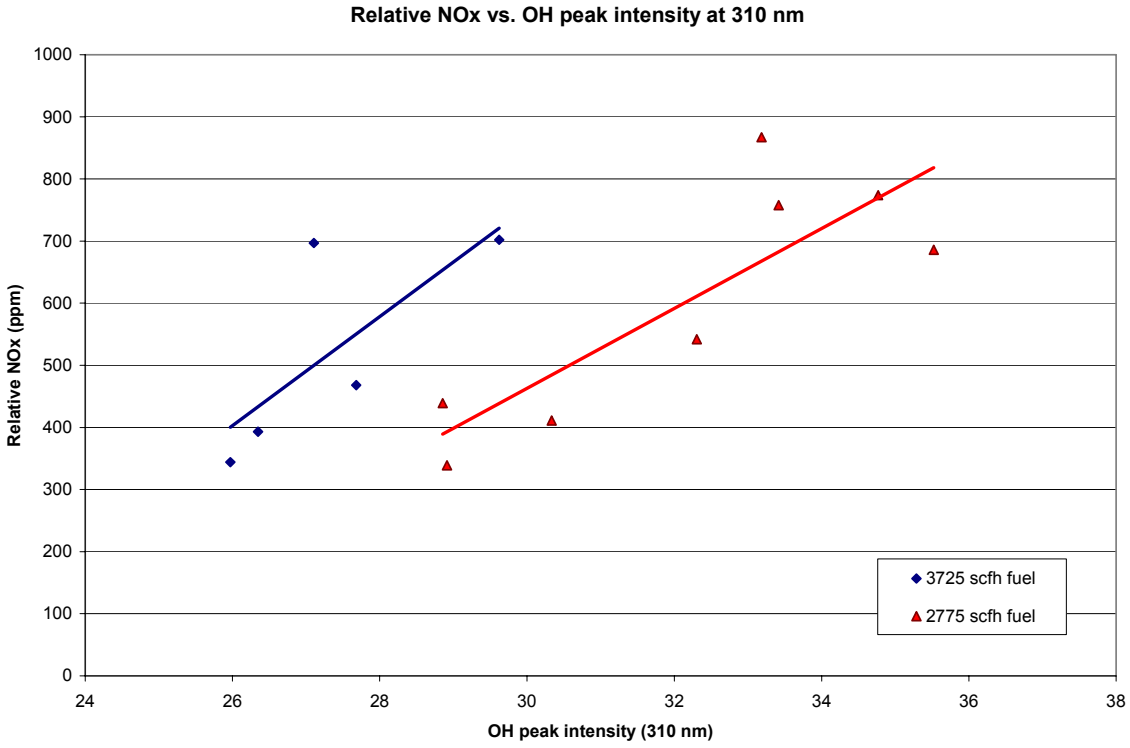

Figure 31. Variation of Relative NOx emission with OH changes at two different heat input

Spectrometer data were collected from one selected burner at various O/F ratios and two heat input conditions at this furnace. The spectrum intensities at a selected range of the visible spectrum were examined to see the impact of the changing O/F ratio in a ramp-up fashion. Figure 32 shows the intensity variation as the O/F changes at two heat input conditions.

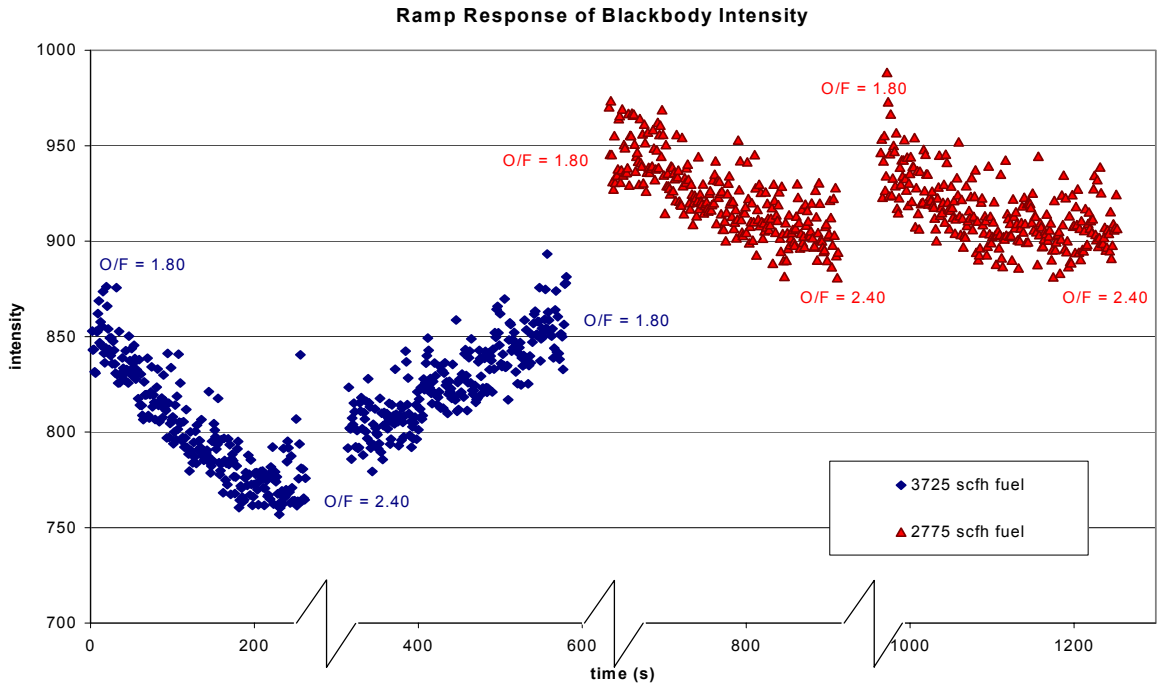

Figure 32. Spectrum intensity response to changing O/F ratio at two heat input conditions

A simulation program using LabView software was developed to show the result of control experimentation using flame image analysis for the multi-burner commercial glass furnace data for demonstration in the commercialization activities. Figure 33 shows a sample of such result. This screen shot from the Labview shows that a flame image characteristic (feature) follows the step change in the natural gas flow rate of an individual burner at this multiburner furnace. The lower plots in this figure show the corresponding spectrum intensities in VIS and UV range.

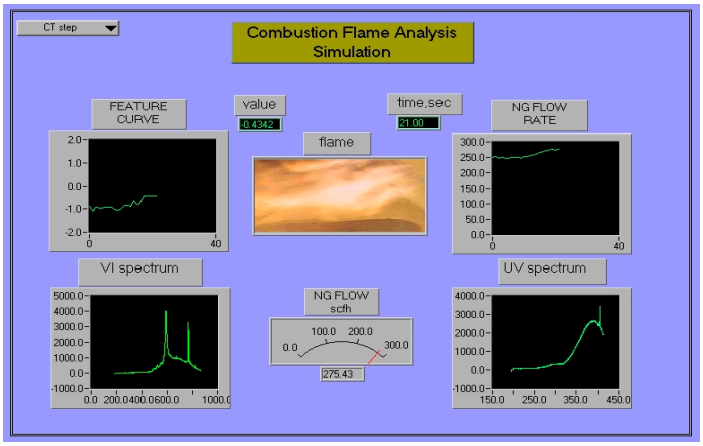

Figure 33. Variation of flame image feature with step changes in gas flow rate

Air/Fuel Commercial Glass Furnce

The air/fuel commercial furnace was a regenerative type rated at 170 Million Btu/hr with a 25 tons/hr of glass production. The furnace is fired in a cyclic mode, with a 20-minutes cycle. When the furnace is fired on one side, the regenerator on this side acts as an air preheating chamber, while the opposite side becomes the flue gas exhauster. Total furnace air flow is drawn into a common windbox for supply to all burners.

Experiments were designed and data acquisitions were completed on two occasions (October 29-30, 2002 and November 19-20, 2002) at this selected commercial glass furnace. Various tests were performed. During these tests, a pair of burners was selected and the air/fuel ratio and heat input rate were changed for these two burners. The maximum fuel flow rate change was only 1.7 percent, which is not a significant change in burner stoichiometry. In addition, a series of tests were performed by changing the overall furnace air/fuel ratio randomly. A portable analyzer was utilized to sample flue gas from a port directly opposed to the test burner. Figure 34 shows the spectrometer and periscope camera set-up at this furnace.

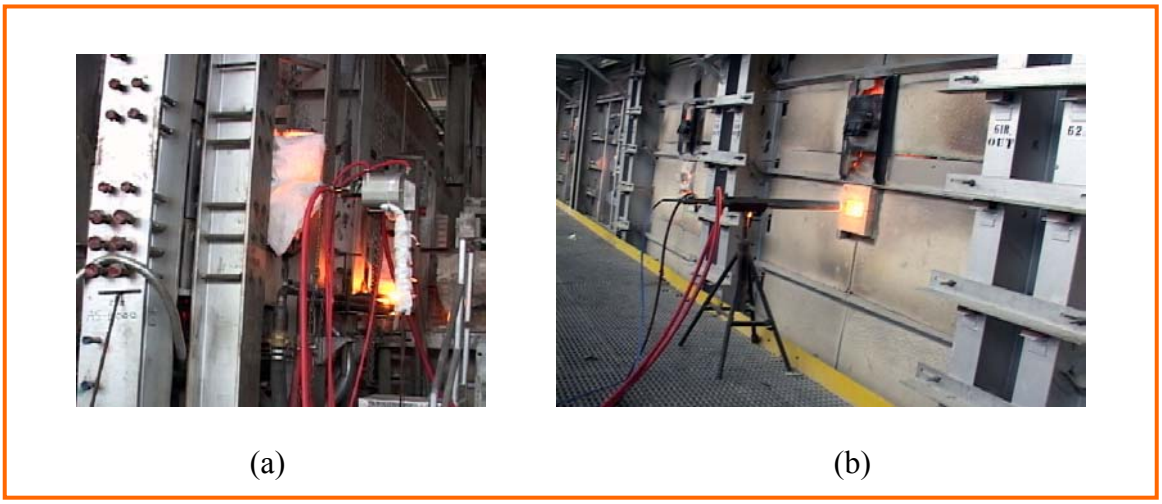

(a) (b)

Figure 34. Set-up for (a) Camera and (b) spectrometer

A sample result of data analysis for temperature calculation for the data collected on November 19-20, 2002 at this commercial plant is presented here. The spectrometer was upgraded to accommodate a trifurcated fiber optics to obtain all three regions UV, VIS, and Near IR (NIR) and compare temperature calculations for VIS and near IR region of spectrum. Figure 35 shows a sample spectrum covering UV, VIS, and NIR region. Figure 36 shows the temperature calculations for VIS and NIR spectrum data using black body radiation model and Tungsten Halogen lamp (3100 K) for calibration. Temperature calculations using VIS region of spectrum show similar trend as compared with NIR region. The discrepancy between the measured temperature by a hand held IR Gun and the calculated temperature is due to Halogen calibration which is at high temperature compared to furnace temperature. To show this point, data from the same furnace are used with a different calibration method and the results are compared with Halogen calibration. Figure 37 shows the results of temperature calculations during the time between the two cycles of the furnace. This figure shows temperature calculations for both VIS

and NIR using a reference calibration much closer to the furnace temperature, as well as, calibration with Tungsten Halogen lamp. The results show that VIS and NIR spectrum provide the same temperature and both are very close to the IR Gun measured temperature. Furthermore, the temperatures calculated using Tungsten Halogen lamp (3100 K) for both VIS and NIR are higher than IR Gun measured temperature (for more details on this subject see publication number 4). Figure 38 shows the excess oxygen variation with NOx.

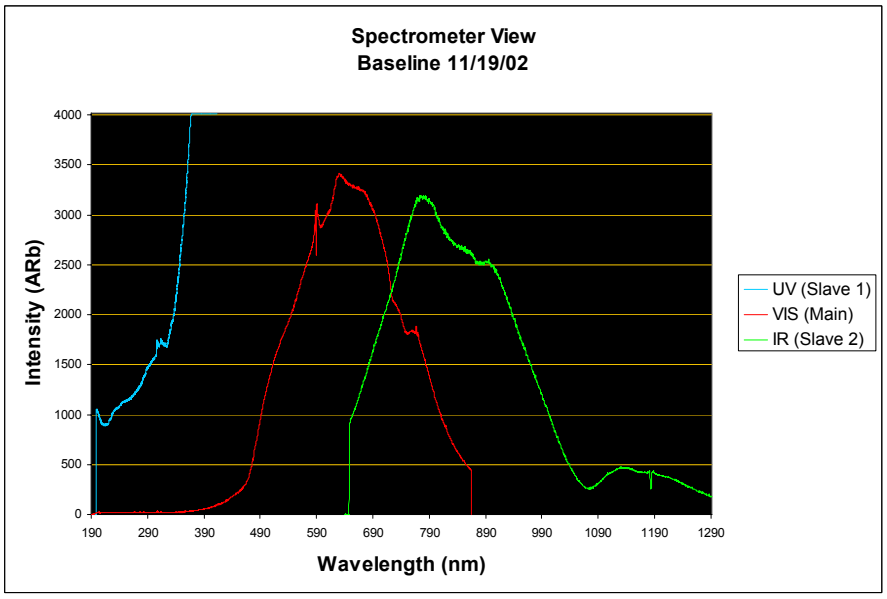

Figure 35. Flame spectrum for UV, VIS, and NIR region from a commercial furnace

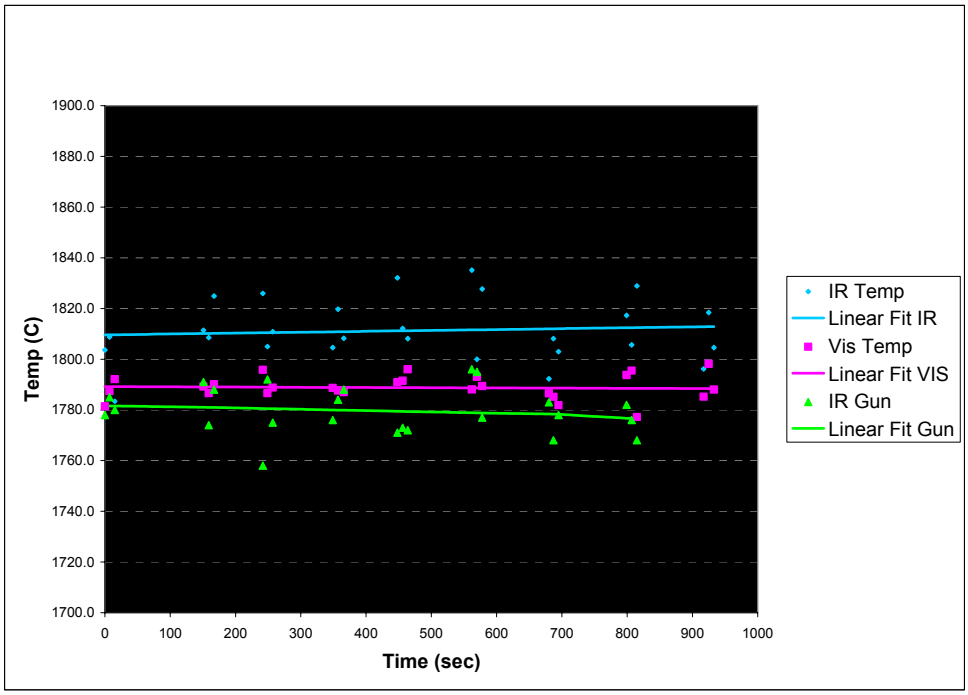

Figure 36. Temperature calculation results using black body model

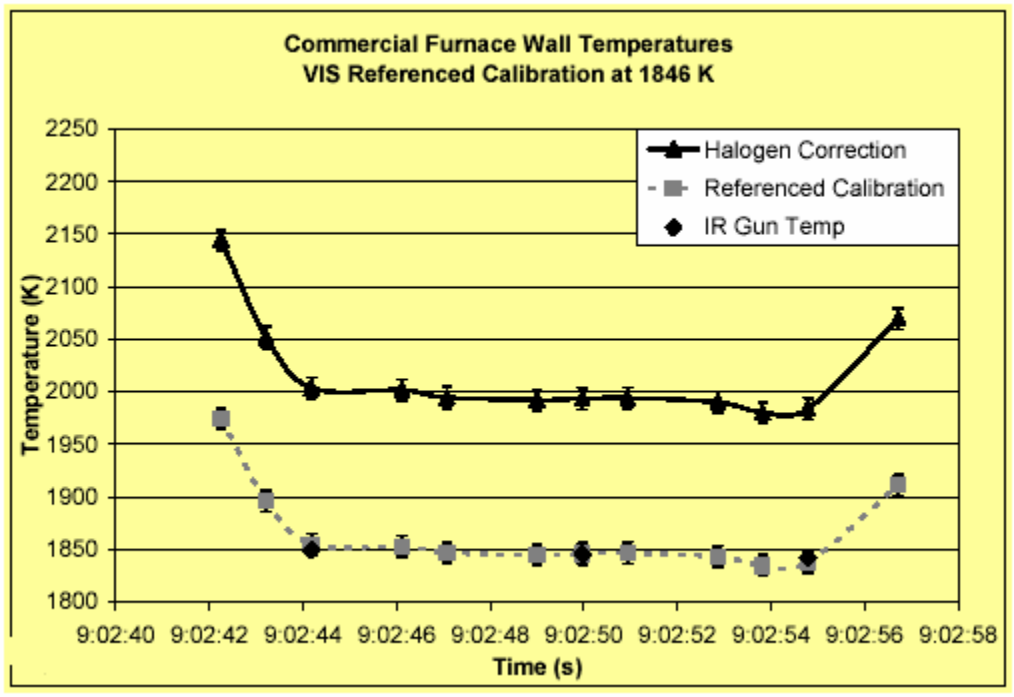

(a)

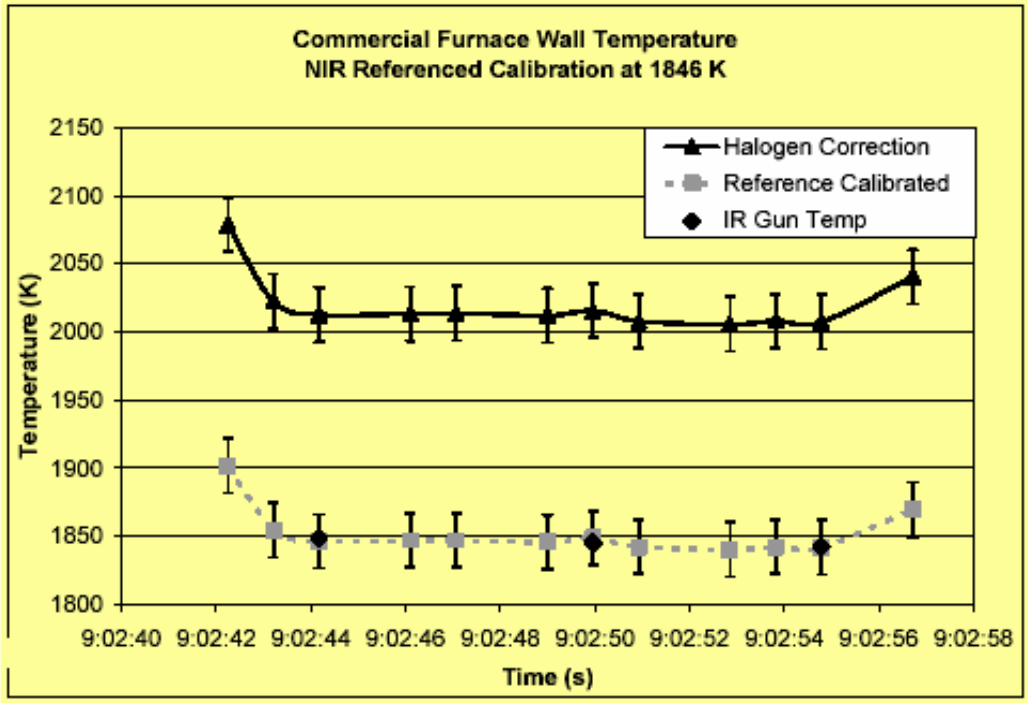

(b)

Figure 37. Calculated temperatures for VIS (a) and NIR (b) spectrum

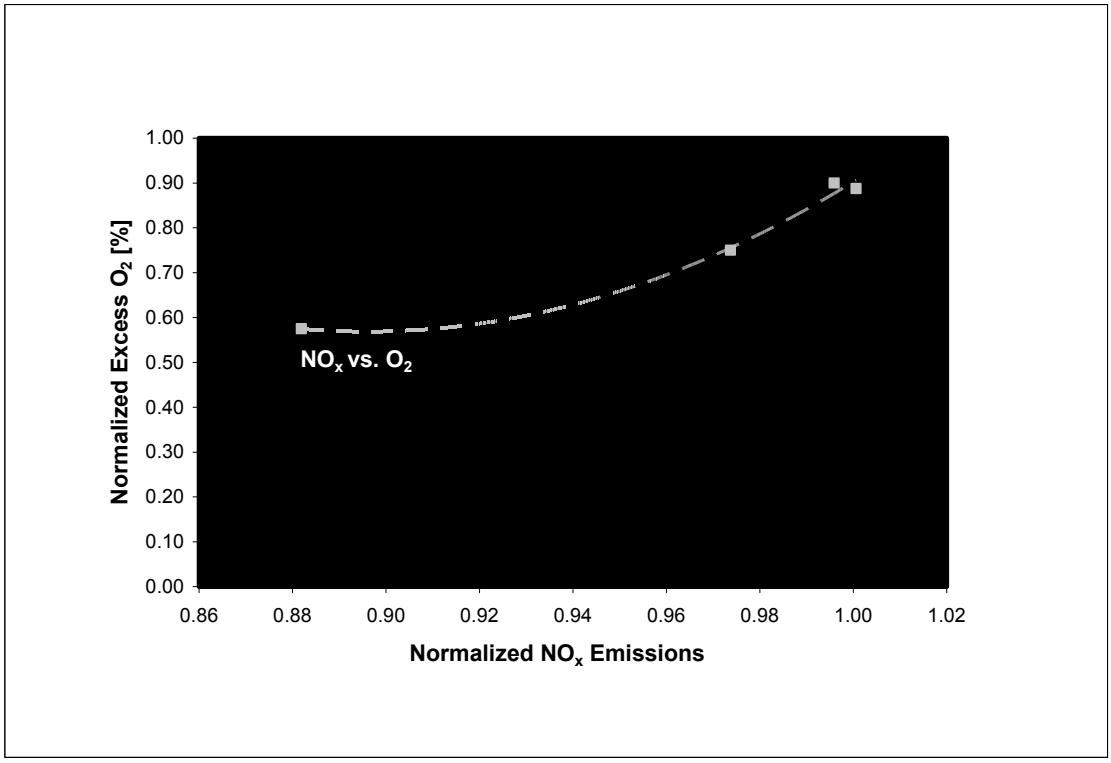

Figure 38. Variations of O_2 with NO_x changes

A sample result of flame image analysis is presented here. Flame images are analyzed frame by frame for two different natural gas flow bias of +500 Scfh and -500 Scfh (less than 1.7% change) at one selected burner. Figure 38 shows how the two combustion conditions at these two natural gas flow are recognized apart through one of the flame image features.

The result of Decision Tree analysis for classification of the flame image data presented in Figure 39 is shown in table 2. The result shows less than 1% error for the total input data of 840. Similar results are obtained when changing the A/F ratio for the same burner under examination.

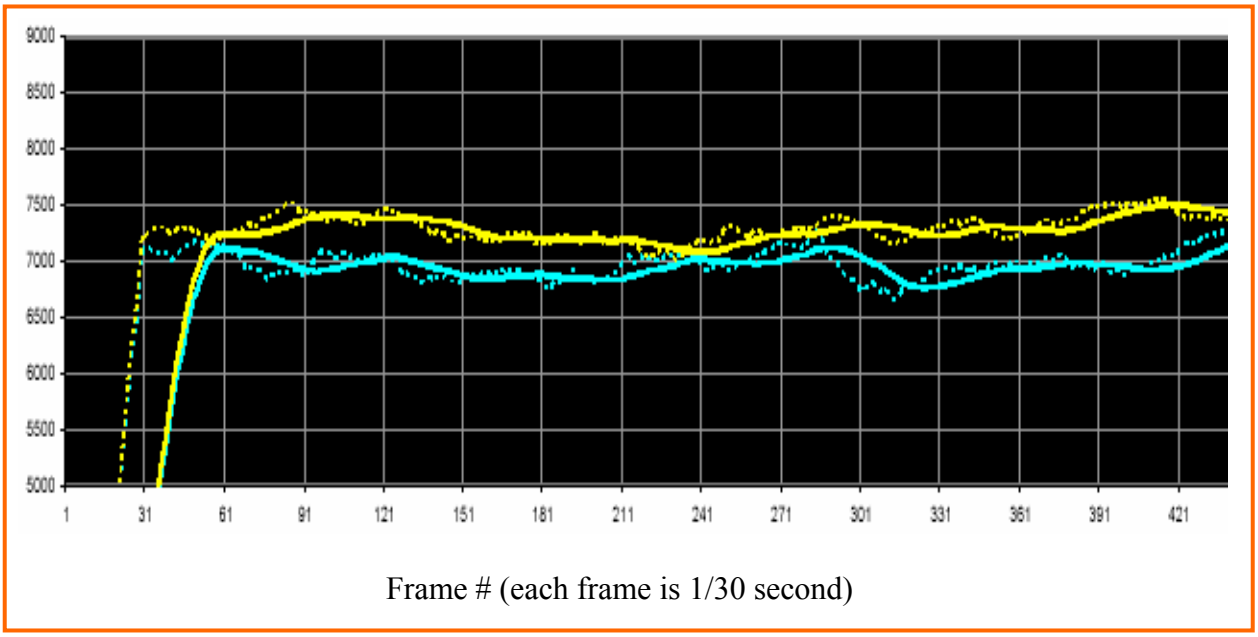

Figure 39. Plot of one flame image feature with a total of 1.7% change in gas flow rate

Table 2. Result of Decision Tree analysis of the flame image data

Input Data type	Number of Input	Correctly Classified	Misclassified
Baseline	292	291	1
NG +500	274	272	2
NG -500	274	269	5

Another activity of the second year of Phase II was to design a user interface for the system. A graphical user interface (GUI) was designed for integration with the control system in a commercial glass furnace. A sample of this GUI screen shots of levels 1&3 are shown in figures 40 and 41. In this design, the first level provides the minimum information for simplicity. Operator can select higher levels for more information as needed.

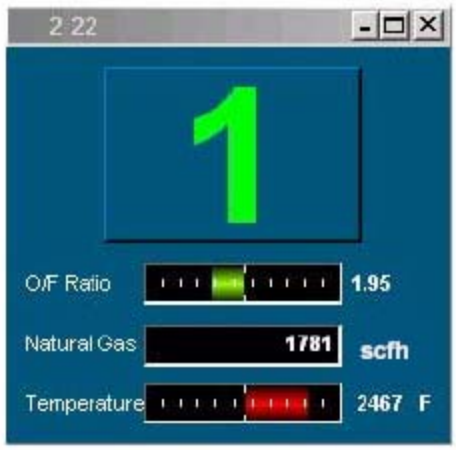

Figure 40. Screen shot for Level 1 for burner #1

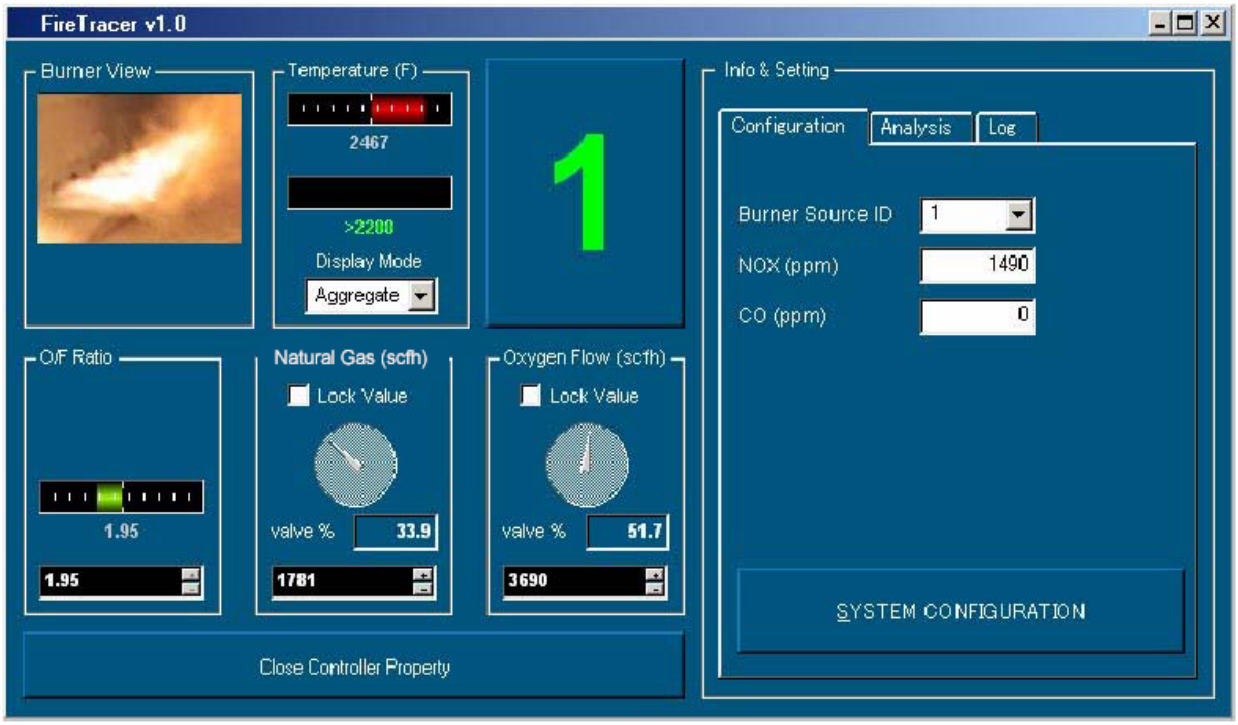

Figure 41. Screen shot for Level 3 for burner #1

SUMMARY OF ACCOMPLISHMENTS DURING THIRD YEAR OF PHASE II

The main activities during the third year of phase II were:

1. Control experimentation at commercial glass furnace for oxy/fuel and air/fuel burner
2. System evaluation at both oxy/fuel and air/fuel commercial furnaces
3. System evaluation for application in gas fired steel reheat furnaces
4. Comparison of temperature calculations in VIS and NIR region of spectrum

A comparison of temperature calculation in VIS and NIR region of spectrum is briefly discussed on page 32-34 in order to compare with similar results in year two of Phase II.

Second data acquisition from an air/fuel multi-burner commercial glass furnace was performed on April 29, 2003. The furnace is fired in a cyclic mode, with a 20-minutes cycle. When the furnace is fired on one side, the regenerator on this side acts as an air preheating chamber, while the opposite side becomes the flue gas exhauster.

New experiments were designed for this data acquisition and system evaluation. Various control experimentations were performed to test the sensitivity and delay in response of the flame monitoring system. Decision Tree was used with 99% success rate to classify various conditions of operations. Figure 42 shows a sample plot of one Flame feature behavior during step-up and step-down changes in natural gas flow rate. Flame feature follows the step changes (orange color, around 6300-7200 fps and 15300-16200 fps in Figure 42) both up and down steps with no time delay. Although, the pink line in figure 42 during the time between frame# 7200 and 15300 should have been a straight line (as no change was made to natural gas flow), due to unanticipated drift in the air flow rate this line is downward.

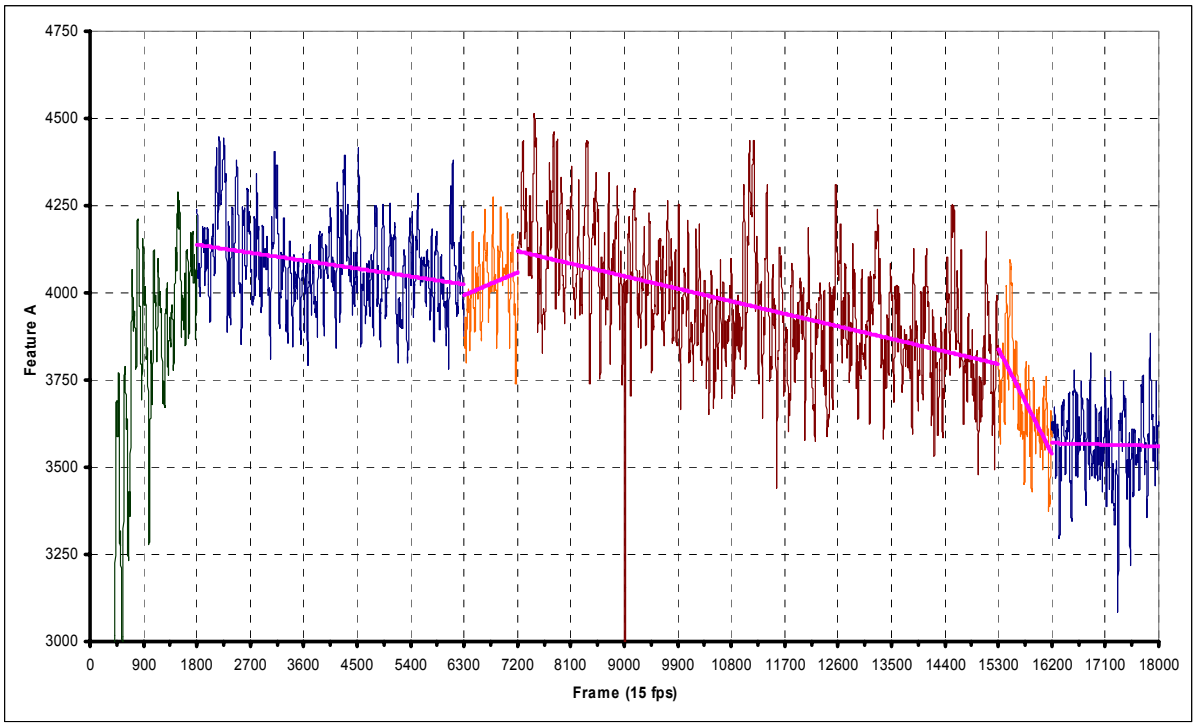

Figure 42. Flame feature behavior during a step-up and step-down change in natural gas flow rate

This report provides successful results of system evaluation for a different type of furnace namely, an air/fuel furnace. The air/fuel commercial furnace was a regenerative type rated at 170 Million Btu/hr with a 25 tons/hr of glass production. With this results, the system evaluation is successfully completed both for oxy/fuel and air/fuel commercial furnaces.

Steel Reheat Furnace

A comprehensive search for selection of an appropriate steel furnace was launched. The final choice was selected based on the furnace/burner design and operating temperature. The selected furnace is a steel reheat furnace with an operating temperature of near 2400 ^{o}F.

New experiments were designed for this data acquisition which was scheduled for October 20-22, 2003. Figure 43 shows one of the furnaces at this plant with eight burners at the top zone and a glowing hot steel log just released from the furnace. Figure 44 shows periscope and spectrometer equipment set-up.

Figure 43. A view of a furnace back wall and a hot steel log output

Figure 44. Periscope and spectrometer set-up in steel reheat furnace

Steel Reheat Furnace Data Analysis

Data acquisition from the selected steel reheat furnace was performed on October 20-22, 2003 with furnace operating temperature ranging over 2300 ^{o}F to 2400 ^{o}F during the experiments and data collection period. The reheat furnaces run three dual (top and bottom) zones: preheat, heating and soak zones. The total maximum heat input for the reheat furnaces is 500 Million Btu/hr.

The burners on these zones are of the diffusion flame type and fired with air and a blend of gaseous fuel that contains coke oven, blast furnace and natural gas. The composition ratio between these gases is constantly changing, depending on gas availability from the nearby coking and blast furnace. Combustion is controlled by a rudimentary feed-forward control system based on a zone temperature control scheme. The prescribed zone temperature set-point is maintained by controlling the total zone fuel flow.

The total combustion air to each zone is handled with a force draft fan and preheated via a tubular preheater installed in the flue gas duct, and measured with two Ventury flow meters (one per air side). The degree of air preheat (which depends on the flue gas temperature and should impact stack nitrogen oxide, NO_x emissions) and air/fuel ratio at the burner level are not controlled. Adjustments are allowed in the control system to modify the percent of air flow, which impose an overall excess air bias to the zone from a hard-coded air/fuel ratio. Visual observations of the combustion conditions are done periodically, however, no on-line monitoring capabilities, like those provided by a permanent periscope, exist at this facility.

A total of six tests were performed with the first series of tests consisting of changes to the zone air bias. In this series, the percentage of total air flow was moved from the 80 percent reference value to the 60 and 100 percent levels. Total fuel flow was maintained constant and temperature set point was at 2300 ^{o}F during these tests. The second series of tests consisted of changes to the zone temperature set point. Temperature levels are averaged from thermocouples located at the furnace walls and kept in the range of 2300 to 2400 ^{o}F. Temperature tests were performed at constant air flow and temperature levels of 2300 ^{o}F, 2350 ^{o}F, and 2400 ^{o}F. No automated data collection exists on these furnaces. For this reason, data was collected manually.

Most of the results obtained from these experiments are indicative of the deficiency of the furnace combustion control system. Figure 45 shows how the fuel supply heating value changes in relation to the flows of coke oven and natural gas. No blast furnace gas was available on the day of these tests. The fuel calorific value is of a typical mid-Btu gas. The figure shows good correlation of the heating value and the amount of natural gas in the mixture, indicating that this gas is used to compensate for the variability of the waste gases. However, the control of the fuel supply is done in terms of the total fuel flow to the zone (increasing the fuel demand as the average zone temperature drops below the temperature set point) and not in terms of the right blending of the gas components, which is not done automatically. This results in a broad range of overall calorific values and, consequently, inefficiently transient combustion conditions.

Figure 45 shows all data points collected during these tests in terms of the on-line calorific value and gas flow rate. Figure 46 indicates that increased levels of heating values result in elevated levels of stack temperature that will result in stack losses, detrimental to the furnace thermal efficiency. In addition, elevated stack temperatures will result in higher levels of air preheat, resulting in higher NO_x emissions.

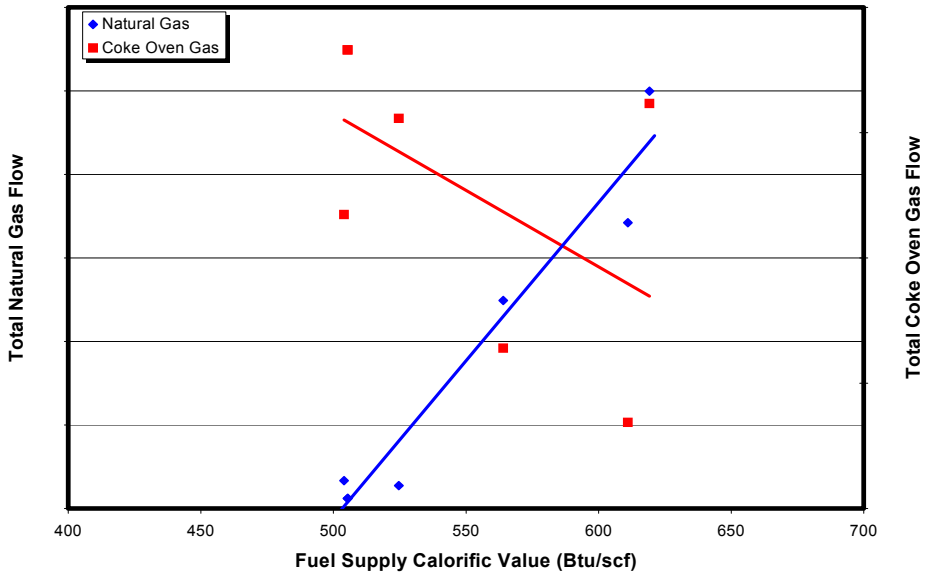

Figure 45. Fuel gas flows and heating value behavior

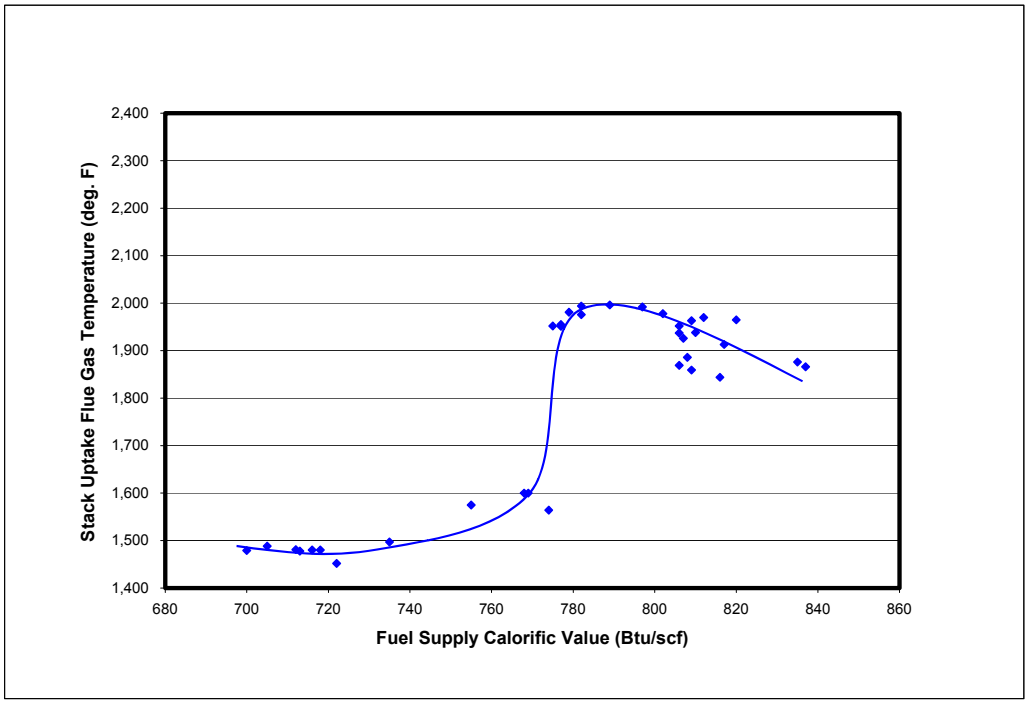

Figure 46. Impact of fuel heating value on combustion temperatures

In terms of the control of the air/fuel ratio, Figure 47 shows a plot of the measured total air to total fuel ratio for the zone of interest, as a function of the percent air flow to this zone, input into the control system. For the three test points shown on the correlated line, the system appears to operate at the indicated ratio, in response to the demanded change. However, these changes were made back-to-back and for short periods of time. When other data points are plotted on the figure, corresponding to different zone temperature set point (but same air bias of 80%) the range of the actual air/fuel ratio spreads from approximately 8 to close to 12, indicating that the burner air/fuel ratio is not well controlled.

The results manifest the shortcomings on combustion control systems typical of these types of aged furnaces. It is evident that good flame control capabilities are needed to have better combustion control and fuel-efficient operation, plus the added benefit of emissions reductions.

Figure 48 shows a sample of feature from this furnace from two experiments at two air/fuel ratios. This plot shows that the two conditions are separable and the concept of flame feature analysis and monitoring works in the same fashion as in glass furnaces.

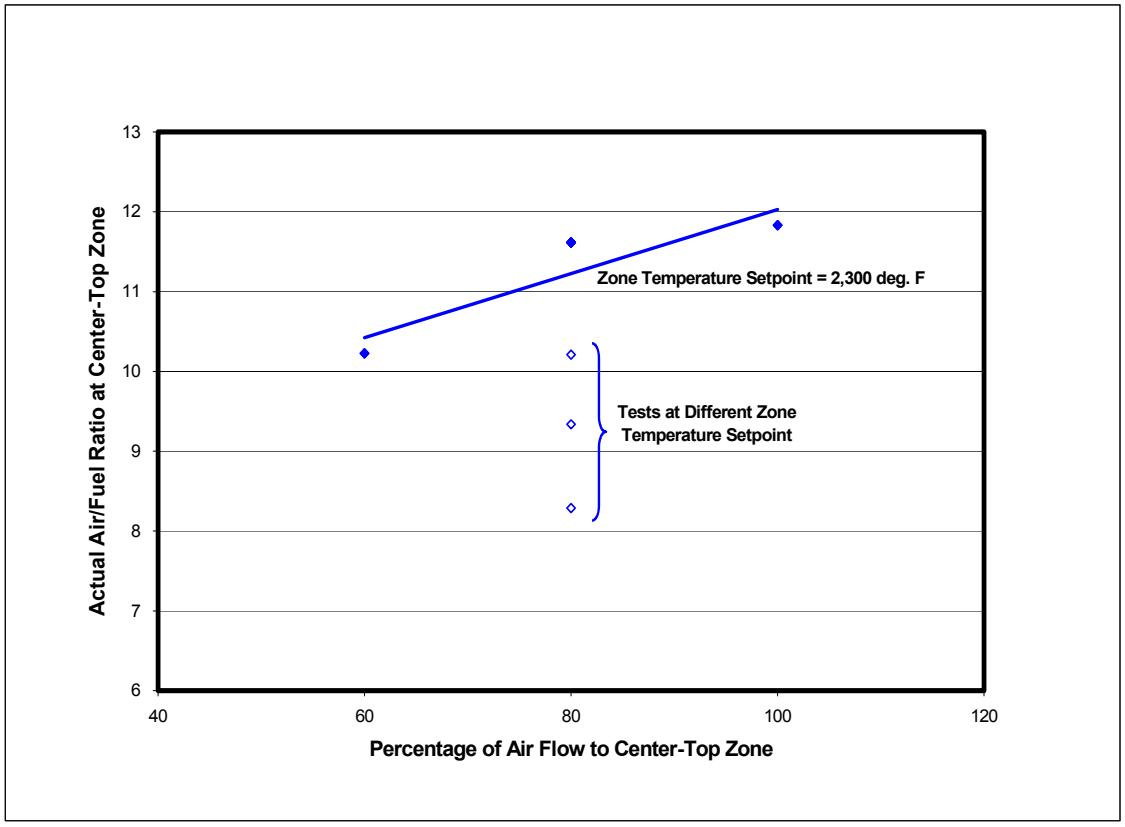

Figure 47. Evaluation of zone Air/Fuel ratio control

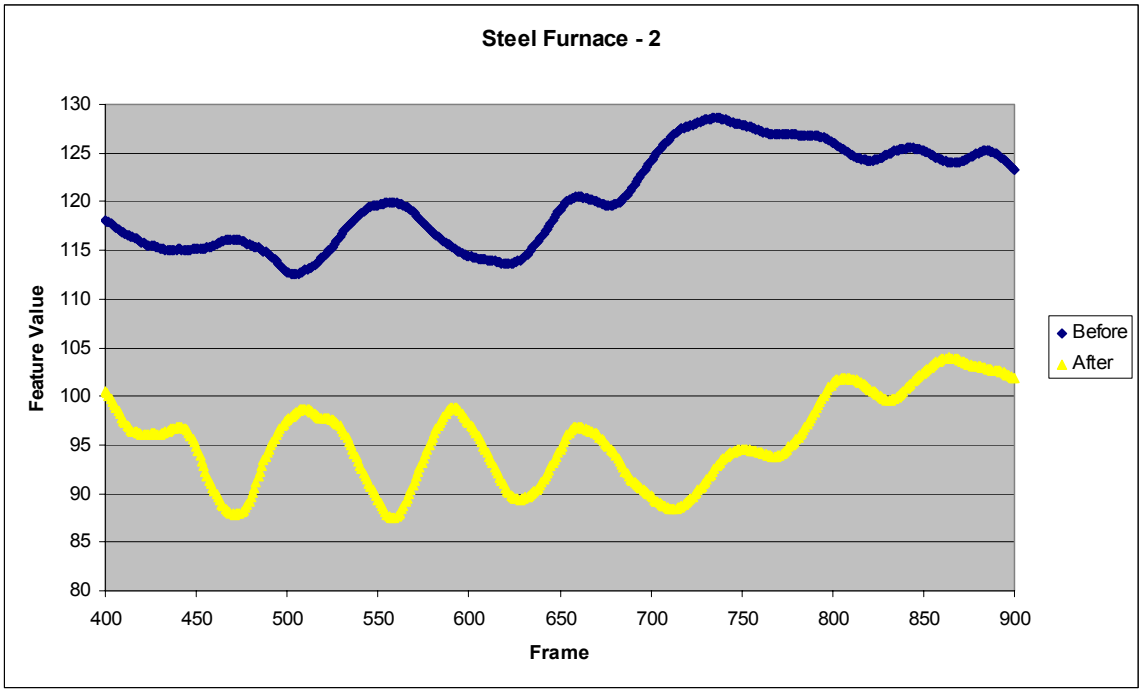

Figure 48. Feature values plotted frame by frame before and after air/fuel ratio change

Data analysis result of this furnace shows the successful application of the developed vision technology to other gas-fired furnaces of the IOF industries. Furthermore, the low efficiency and the magnitude of energy consumption (500 Million Btu/hr for one 3-zoned furnace) as compared to a typical medium size glass furnace (80 Million Btu/hr) indicate the suitability of this industry (gas-fired furnaces in the steel industry) for implementation of the system developed here.

SUMMARY OF ACCOMPLISHMENTS DURING THE FOURTH YEAR OF PHASE II

During the fourth year of phase II of this project the focus was on prototype development and beta testing and evaluation of the prototype.

The periscope camera was upgraded with an advanced camera thus avoiding the use of the older technology of frame grabbing as an intermediate step for converting the camera image to frames that are then analyzed by the sensor software. With this upgrade, images are fed directly into a computer and the system software in real time.

The use of the newly introduced camera technology will reduce the cost to industry of the final sensor system, as frame grabbers are expensive and are camera-dependent. This will also provide additional flexibility for selecting the most appropriate camera for a specific furnace setting.

Several tests were performed at a glass manufacturing company on March 23-24, 2004. The following activities were carried out:

- Calibrate and fine-tune the sensor software to work in a new furnace and from a new camera location.
- Batch-line detection of the sensor was compared with visual observation by furnace operator to verify sensor sensitivity and superiority over operator visual observation.
- Temperature calculations were evaluated by comparison with other optical detectors such as IR gun as well as thermocouples.

After evaluation of the new camera image capturing performance, it was concluded that a higher resolution but lower frame rate camera was more appropriate. A camera was ordered on April 12, 2004.

Prior to going to the glass furnace, laboratory tests were performed with this new camera to check the camera and its associated control software at the University of Missouri-Columbia coal fired boiler. Figure 49 shows the camera and spectrometer set-up at this boiler. Figure 50 shows one image focusing on the boiler wall for temperature calculations. The camera and its control software were tested and the performance for both "still" imagery and video capturing was evaluated. Various lighting control through camera software were also examined.

The last test and evaluation took place on October 11-12, 2004. Figure 51 shows both camera/periscope and the associated PC/monitor in operation as this test was fully on-line / real-time for performance evaluation of both batch-line sensor and 3-D temperature sensor. Some data was also acquired for off-line analysis.

The following activities were carried out during this test:

- Configuring the camera software to adapt to the furnace lighting condition.
- Real-time Batch-line detection of the sensor and comparison with visual observation.
- Real-time temperature calculations, as well as, evaluation by comparison with other optical detectors such as IR gun, pyrometers, and thermocouples.
- Testing different locations at the furnace for camera installation for optimizing visualization capabilities.

Figure 49. Side by side Periscope & Spectrometer set-up at the coal boiler

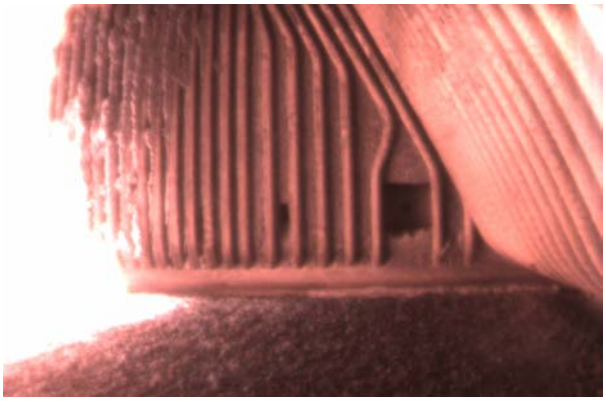

Figure 50. Sample image of inside of the coal boiler

Figure 51. Periscope (inside red box) & PC/Monitor set-up at the host furnace

Conclusions

The final products/sensors that emerged from this project so far have exceeded the original goal. The following three sensors are developed:

1. Flame Sensor with two major capabilities: a) virtual flame detector to detect a non-firing burner, and a flame monitor with adjustable memory, and b) Flame analyzer to provide the status of combustion of a burner.

2. Temperature Profiler (providing 3-D temperatures of furnace walls and crown)

3. Batch-line Detector for glass melting furnaces (to measure distance from furnace wall to the line of feed and melt separation)

The implementation of the batch-line and temperature sensors in real time will lead to advanced level furnace control as well as batch-line and temperature monitoring. This would lead to optimization in energy savings when integrated with the furnace control system.

In addition, two objectives were achieved as a result of verification and validation activities in the last year of Phase II, namely bringing sensors to advanced status with upgraded camera as well as introducing direct frame capturing in real time and reducing the required equipment cost to industry.

The sensors can be integrated into a furnace control system in real time or utilized as a diagnostic tool for manual control adjustment by an operator.

Publications/Presentations:

1. Ph.D. dissertation: "Blackbody Temperature Calculations from Visible and Near IR Flame Spectra for Natural Gas-Fired Furnaces" by Rodney Rossow, University of Missouri-Columbia, July 2005.

2. M.S. thesis: "Spectroscopic Measurements in Flames for Glass Furnace Applications" by Michael Saeger, Lehigh University, 2002.

3. M.S. thesis entitled "Digital Analysis of Flame Images for a Natural Gas fired Furnace" by Huihao Fan, University of Missouri-Columbia, May 2003.

4. Keyvan, S. Rossow, R., Romero, C., "Blackbody-based Calibration for Temperature Calculations in Visible and Near-IR using a Spectrometer," Fuel Journal, Vol. 85/5-6 pp 796-802, 2006.

5. Keyvan, S., Rossow, R., Romero, C., Li, X., "Comparison between Visible and Near-IR Flame Spectra from Natural Gas-Fired Furnace for Blackbody Temperature Measurements," Fuel Journal, Vol. 83/9 pp 1175-1181, 2004.

6. Romero, C., Li, X., Keyvan, S., Rossow, R., "Spectrometer-Based Combustion Monitoring For Flame Stoichiometry and Temperature Control," Applied Thermal Engineering journal, Vol. 25, issue 5-6, pp 659-676, 2004.

7. Keyvan, S., Rossow, R., Velez, M., Headrick, W., Moore, R., Romero, C., "Combustion Control Experimentations at a Pilot Scale Glass Furnace" Environmental Issues and Waste Management Technologies in the Ceramic and Nuclear Industries, IX Ceramic Transactions Volume 155, 2003.

8. Keyvan, S., Presentation at the Center for Glass Research (CGR) semi-annual meeting, June 19, 2002 in Rolla Missouri.

9. Keyvan, S., "Flame Image Analysis for Diagnostics and Control in Gas Fired Furnaces," Proceedings of American Flame Research Committee (AFRC) annual meeting, Houston, Texas, November, 2002.